

Comparison of Nuclear Fuels for TREAT: UO_2 vs U_3O_8

Michael V. Glazoff,
Isabella J. van Rooyen,
Benjamin D. Coryell, and
Clemente J. Parga

April 2016



The INL is a U.S. Department of Energy National Laboratory
operated by Battelle Energy Alliance

DISCLAIMER

This information was prepared as an account of work sponsored by an agency of the U.S. Government. Neither the U.S. Government nor any agency thereof, nor any of their employees, makes any warranty, expressed or implied, or assumes any legal liability or responsibility for the accuracy, completeness, or usefulness, of any information, apparatus, product, or process disclosed, or represents that its use would not infringe privately owned rights. References herein to any specific commercial product, process, or service by trade name, trade mark, manufacturer, or otherwise, does not necessarily constitute or imply its endorsement, recommendation, or favoring by the U.S. Government or any agency thereof. The views and opinions of authors expressed herein do not necessarily state or reflect those of the U.S. Government or any agency thereof.

Comparison of Nuclear Fuels for TREAT: UO_2 vs U_3O_8

**Michael V. Glazoff, Isabella J. van Rooyen, Benjamin D. Coryell, and
Clemente J. Parga**

April 2016

**Idaho National Laboratory
Idaho Falls, Idaho 83415**

<http://www.inl.gov>

**Prepared for the
U.S. Department of Energy
Office of Nuclear Energy
Under DOE Idaho Operations Office
Contract DE-AC07-05ID14517**

INTENTIONALLY BLANK

Comparison of Nuclear Fuels for TREAT: UO₂ vs U₃O₈

**INL/EXT-16-37972
Revision 0**

April 2016

Approved by:

I.J. van Rooyen
TREAT Conversion LEU Fuel Engineering and Design Lead

Date

S.R. Morrell
TREAT Conversion Program Manager

Date

INTENTIONALLY BLANK

ABSTRACT

The Transient Reactor Test (TREAT) facility that resides in the Materials and Fuels Complex (MFC) at Idaho National Laboratory (INL) first achieved criticality in 1959, and successfully performed many transient tests on nuclear fuel until 1994 when its operations were suspended¹. Resumption of operations at TREAT was approved in February 2014 to meet the U.S. Department of Energy Office of Nuclear Energy objectives in transient testing of nuclear fuels. The National Nuclear Security Administration's Office of Material Management and Minimization is converting TREAT from its existing highly enriched uranium core to a new core containing low-enriched uranium (i.e., U-235 < 20% by weight).¹

The TREAT Conversion Project is currently progressing with conceptual design phase activities. It is very important to make the right decision on what type of nuclear fuel will be used at TREAT. In particular, one has to consider different oxides of uranium and, most importantly, UO_2 vs U_3O_8 .¹ The objective of this report is to evaluate and compare the differences and similarities between these two uranium oxides: thermodynamic behavior at atmospheric and sub-atmospheric pressure (crystal structure, phase stability, red-ox reactions), some thermo-physical properties (heat conductivity and volumetric expansion, densification during fabrication), chemical reactivity with fuel constituents during fabrication and in contact with assembly materials (zirconium-based cladding) at operational environments (steady-state and planned transients), and design basis accident scenario (reactivity accident transient).

In this report, the results are documented pertaining to the choice mentioned above (UO_2 vs U_3O_8). The conclusion in favor of using UO_2 was made based on the analysis of historical data, up-to-date literature, and self-consistent calculations of phase equilibria and thermodynamic properties in the U-O and U-O-C systems. The report is organized as follows: first, the criteria that were used to make the choice are analyzed, and secondly, existing historical data and current literature are reviewed. This analysis was supplemented by the construction and examination of the U-O and U-O-C phase diagrams in design operation conditions. Finally, the conclusion in favor of the UO_2 down selection is summarized and explained.

INTENTIONALLY BLANK

CONTENTS

ABSTRACT.....	vi
1. INTRODUCTION AND CRITERIA USED FOR UO_2 VS U_3O_8 SELECTION.....	1
2. THERMODYNAMICS AND KINETICS OF URANIUM OXIDES	5
3. POTENTIAL INTERACTIONS INSIDE NUCLEAR FUEL (UO_2 AND U_3O_8 REACTING WITH GRAPHITE)	11
3.1 Uranium Dioxide UO_2 vs U_3O_8 – General Considerations for Graphite Reactions	11
4. AIR INGRESS AND ITS INFLUENCE UPON UO_2 FUEL STOICHIOMETRY AND ZIRCONIUM-BASED CLADDING	22
5. VOLUMETRIC CHANGES DURING FUEL BLOCK MANUFACTURING (950°C) AND DURING SUBSEQUENT OPERATION UP TO 820°C.....	23
6. OPTIMAL MANUFACTURING CONDITIONS	25
7. THERMAL CONDUCTIVITY OF UO_2 AND U_3O_8	26
8. INTERACTIONS OF NUCLEAR FUEL WITH CLADDING MATERIAL	27
9. ACKNOWLEDGEMENTS	30
10. CONCLUSIONS	30
11. REFERENCES	31

FIGURES

Figure 1. Crystalline lattices of UO_2 (left) and U_3O_8 (right). ⁶	3
Figure 2. Bulk fuel density vs. oxygen content for uranium oxides sintered at 1450°C for 2 hours in argon. ^{3,18}	3
Figure 3. Variation of total thermal conductivity as a function of temperature and linear thermal expansion coefficient of UO_2 with temperature. ⁷	4
Figure 4. Variation of the UO_2 creep rate with and without irradiation. ^{3,4}	5
Figure 5. The calculated U-O phase diagram. ¹³	8
Figure 6. The U-O phase diagram according to Reference 14, calculated.....	9
Figure 7. The U-O phase diagram constructed experimentally. ¹⁵	10
Figure 8. Isothermal cross-section of the U-C-O phase diagram. ¹⁶	11
Figure 9. Variation of total thermal expansion and linear thermal expansion coefficient of UO_2 with temperature. ^{3,18}	23

Figure 10. Thermal conductivity of un-irradiated polycrystalline $\text{UO}_{2.00}$. ²⁴	26
Figure 11. Thermal conductivity of U_3O_8 corrected to 100% theoretical density as a function of temperature according to different data; (•) present data. ²⁷	26
Figure 12. Temperature dependence of the phase composition for the alloy Zy-2.	28
Figure 13. Temperature dependence of the phase composition for zircaloy-4.	28
Figure 14. Temperature dependence of the phase composition for ZIRLO TM .	29
Figure 15. Temperature dependence of the phase composition for the alloy M5 TM .	29
Figure 16. Temperature dependence of the phase composition for the alloy Zircaloy-3 (our calculations).	30

TABLES

Table 1. Some Nuclear and Physical Properties of UO_2 and U_3O_8 . ^{4,18}	2
Table 2. Gibbs free energy for the reaction $3\text{UO}_2 + \text{O}_2 = \text{U}_3\text{O}_8$ as a function of temperature at pressure $P=0.05$ mbar, corresponding to the optimal conditions determined at ANL. ⁹	6
Table 3. Values of Gibbs free energy for the reaction $3\text{UO}_2 + \text{O}_2 = \text{U}_3\text{O}_8$ as a function of temperature at ambient pressure $P=1013.25$ mbar (or ~ 1 atm). This Table also illustrates polymorphic transformations that take place at 210°C for $s1 \rightarrow s2$; at 397°C for $s2 \rightarrow s3$; and at 557°C for $s3 \rightarrow s4$ (our calculations).	7
Table 4. Gibbs free energy as a function of temperature for the reaction $\text{UO}_2 + \text{C} = 2\text{CO} + \text{U}$ at ambient pressure (101.325 kPa = 1013.25 mbar ~ 1 MPa).	12
Table 5. Values of Gibbs free energy for the reaction $\text{UO}_2 + \text{C} = 2\text{CO} + \text{U}$ as a function of temperature at external pressure of 0.05 mbar.	13
Table 6. Values of Gibbs free energy for the reaction $\text{UO}_2 + 4\text{C} = \text{UC}_2 + 2\text{CO}$ as a function of temperature at ambient pressure $P=1013.25$ mbar (or ~ 1 atm).	14
Table 7. Values of Gibbs free energy for the reaction $\text{UO}_2 + 4\text{C} = \text{UC}_2 + 2\text{CO}$ as a function of temperature at ambient pressure $P=0.05$ mbar .	15
Table 8. Values of Gibbs free energy for the reaction $\text{UO}_2 + 4\text{C} = \text{UC}_2 + 2\text{CO}$ as a function of temperature at $P=0.01$ mbar.	16
Table 9. Values of Gibbs free energy for the reaction $\text{UO}_2 + 4\text{C} = \text{UC}_2 + 2\text{CO}$ as a function of temperature at $P=0$.	17
Table 10. Values of Gibbs free energy for the reaction $\text{U}_3\text{O}_8 + 8\text{C} = 3\text{U} + 8\text{CO}$ as a function of temperature at ambient pressure $P=1013.25$ mbar (or ~ 1 atm).	18
Table 11. Values of Gibbs free energy for the reaction $\text{U}_3\text{O}_8 + 8\text{C} = 3\text{U} + 8\text{CO}$ at $P=0.05$ mbar.	19
Table 12. Values of Gibbs free energy for the reaction $\text{U}_3\text{O}_8 + 8\text{C} = 3\text{U} + 8\text{CO}$ at $P=1$ atm.	20
Table 13. Values of Gibbs free energy for the reaction $\text{U}_3\text{O}_8 + 8\text{C} = 3\text{U} + 8\text{CO}$ at $P=0.05$ mbar.	21
Table 14. Values of Gibbs free energy for the reaction $\text{U}_3\text{O}_8 + 8\text{C} = 3\text{U} + 8\text{CO}$ at $P=0$.	22
Table 15. Coefficients of thermal expansion of the MOX fuel and stoichiometric $\text{UO}_{2.00}$. ²³	24

Comparison of Nuclear Fuels for TREAT: UO_2 vs U_3O_8

1. INTRODUCTION AND CRITERIA USED FOR UO_2 VS U_3O_8 SELECTION

There is a major effort underway for limiting or eliminating the international trafficking of highly enriched uranium (HEU). For solving this problem, the Reduced Enrichment for Research and Test Reactors (RERTR) Program was started in 1978 by the U.S. Department of Energy (DOE) to develop technology needed to convert HEU to low-enriched uranium (LEU) fuels. LEU is supposed to contain less than 20% of the ^{235}U isotope and, therefore, is much more resistant to proliferation.

Among other things, nuclear fuel for a research reactor must possess the following properties:

1) High value of thermal flux; and 2) Density of the LEU fuel must also be high.

This second goal can be achieved typically via two approaches: a) Increase the loading of the fuel in the fuel element ; or b) Change the fuel composition to one that contains more fissile uranium isotope(s). To convert all considered reactors to LEU fuels, a density of at least 8 g-U/cm^3 will be generally required.⁴ From this perspective, consider dispersion fuels and monolithic fuels. A typical dispersion consists of the fuel in powder form dispersed, for example, in a graphite matrix that is clad between cover plates, e.g., made of Zircaloy-4 or M-5TM zirconium-based cladding alloys that are being considered for the Idaho National Laboratory (INL) Transient Reactor Test (TREAT) facility.¹ The highest possible uranium loading can be achieved for some U-Mo alloys: 17.0 g/cm^3 with U-10Mo 17.5 g/cm^3 with U-7Mo.⁴ However, for many older experimental reactors ceramic uranium based fuel remains the main choice because its properties have been studied extensively and it possesses a number of well-known advantages over metallic fuels (higher melting point, chemical inertness, property isotropy, and reduced probability of re-criticality during core meltdown).

A very detailed analysis of the different types of fuel was conducted by van Rooyen et al. in their recent Trade Study.¹ The choice was made in favor of the uranium (U-235) based ceramic fuel dispersed in the graphite matrix, so it is necessary at this stage to determine, which of the oxides of uranium (i.e., UO_2 vs U_3O_8) would perform better under the specific conditions of the TREAT reactor. In so doing, we will consider only the most suitable ceramic fuel enriched with U-235 isotope (rather than U-233), although there should not be any difference in the chemical behavior of both isotopes and their respective oxides.

In the Oak Ridge National laboratory (ORNL) earlier work addressing the issue of safe storage of nuclear fuel, the problem of thermal stabilization of the fuel was considered.⁵ The authors noted that the temperature of the process was chosen mostly upon the basis of eliminating residual moisture and volatile impurities. It was concluded that conversion to U_3O_8 was sufficient to accomplish all of the desired goals. The preferred storage form is U_3O_8 because it is more stable than UO_2 or UO_3 in oxidizing atmospheres. Heating in an oxidizing atmosphere at 750°C for at least one hour will achieve the thermal stabilization desired.⁵

Also, the U_3O_8 oxide form had been utilized at TREAT earlier, before the restart efforts were initiated.¹ It is possible that the choice of U_3O_8 was made to ensure there is not any fuel oxidation (and, therefore, dimensional instabilities) associated with the operations of the TREAT.

The prevalent species of uranium oxide are the chemical forms UO_2 , UO_3 , and U_3O_8 , although a number of other phases such as UO ; U_4O_9 ; U_3O_7 and a number of non-stoichiometric phases are also described.

In the literature, it is stated that UO is the lowest oxide (U^{+2} oxidation state) that can be identified only in thin films (native oxide) when uranium is exposed briefly to open air.⁴ It is also well established that the uranium dioxide, UO_2 , can exist in a wide range of variable compounds depending on the temperature, environment, and especially the pressure. The U_3O_7 oxide is formed as a result of the phase transformation reaction⁴:



It forms at a temperature of approximately 150°C, and transforms to U_3O_8 at around 375°C. In its turn, the U_3O_8 oxide is unstable above 450°C and converts back to UO_2 at higher temperatures. This sequence of phase reactions (taking place at different temperatures) can be illustrated as follows⁴:



A major issue about the UO_2 dioxide is that, depending upon temperature and oxygen pressure in the system, it can deviate from its stoichiometric composition in both directions – towards deficiency and excess of oxygen in the crystalline lattice. If the oxygen to uranium atom ratio is 2.0, the UO_2 is stoichiometric. If an oxygen-deficient or excessive uranium exists (i.e., $O/U < 2.0$), the fuel is called super-stoichiometric fuel (UO_{2-x}). If an $O/U > 2.0$, $UO_{(2+x)}$ is called hypo-stoichiometric fuel (x is a small fraction).⁶

The departures from stoichiometry - self-diffusion in fuel itself and inter-diffusion between fuel and cladding materials to form hyper-stoichiometric or hypo-stoichiometric fuel during the reactor operation - could result in deterioration of the UO_2 creep properties. Some nuclear and physical properties of UO_2 and U_3O_8 , the only two uranium oxides that are used for fuel development and/or safe storage, are presented in Table 1.

Table 1. Some Nuclear and Physical Properties of UO_2 and U_3O_8 .^{4,18}

COMPOUND	NUCLEAR PROPERTIES, THEORETICAL (TD) (NATURAL URANIUM)			CRYSTAL STRUCTURE UNIT CELL LATTICE PARAMETER			MELTING POINT (°C)	THEORETICAL OR X-RAY DENSITY (g/ cm³)	URANIUM CONTENT		3
	MACROSCOPIC CROSS SECTION (0.025 eV), cm²/cm³		n ^a	TYPE	(Å)	MOLECULES PER UNIT CELL			(a/o)	(w/o)	
	FISSION Σ _f	ABSORPTION Σ _a									
UO ₂	0.102	0.185	1.34	FCC(CaF ₂ type)	a = 5.468	4	2780	10.96	33.3	88.15	50
U ₃ O ₈	0.065	0.120	1.34	Orthorhombic	a = 6.70 b = 11.94 c = 4.14	2	2500	8.39	27.2	73.61	

From Table 1, it is clear that the nuclear properties of both oxides are quite similar (fission and neutron absorption cross-sections). However, the melting point of UO_2 is somewhat higher (2780°C vs 2500°C). Also, the UO_2 has crystalline structure of the CaF₂ type (*cF12*; FCC –face centered cubic), while U_3O_8 – orthorhombic with different values of all the three lattice parameters a , b , and c . This causes an undesirable anisotropy of properties for U_3O_8 . It might not represent a significant impediment for the safe storage of nuclear fuel, but for its use inside a nuclear reactor as a fuel might be problematic because of the dimensional instability issues. The crystalline lattices of both oxides are presented in Figure 1.⁶

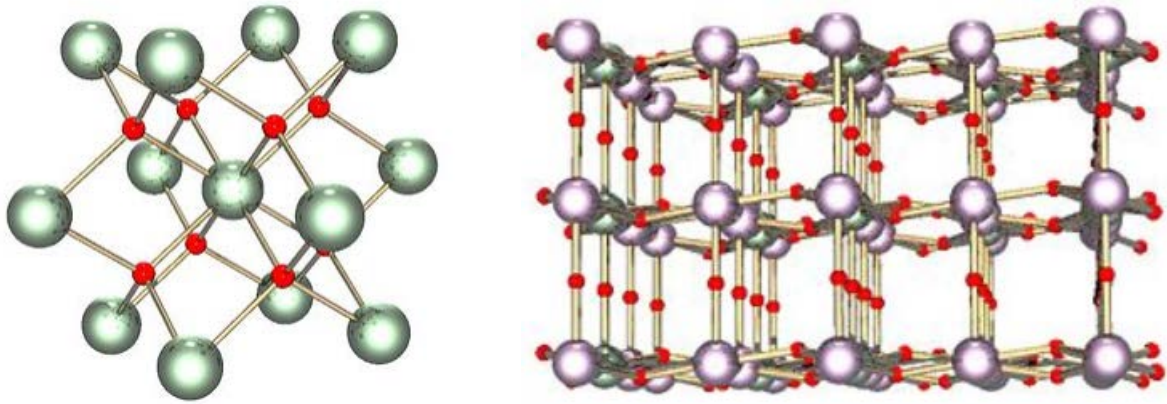


Figure 1. Crystalline lattices of UO_2 (left) and U_3O_8 (right).⁶

Continuing the analysis of Table 1, UO_2 has both higher atomic density and actual density compared to U_3O_8 (10.96 g/cm^3 vs 8.39 g/cm^3). The nuclear fuel fabricated with UO_2 provides a number of advantages for UO_2 compared to U_3O_8 : (a) higher uranium density, (b) high value of thermal conductivity, (c) high capability to contain and retain fission product gases in the fuel and d) high value of linear power rating (q) of the fuel element^{3,4}:

$$q = \int k(T, \rho) dT$$

In terms of the bulk nuclear fuel density and its dependence upon the UO_2 stoichiometry, the following results were reported^{3,4}:

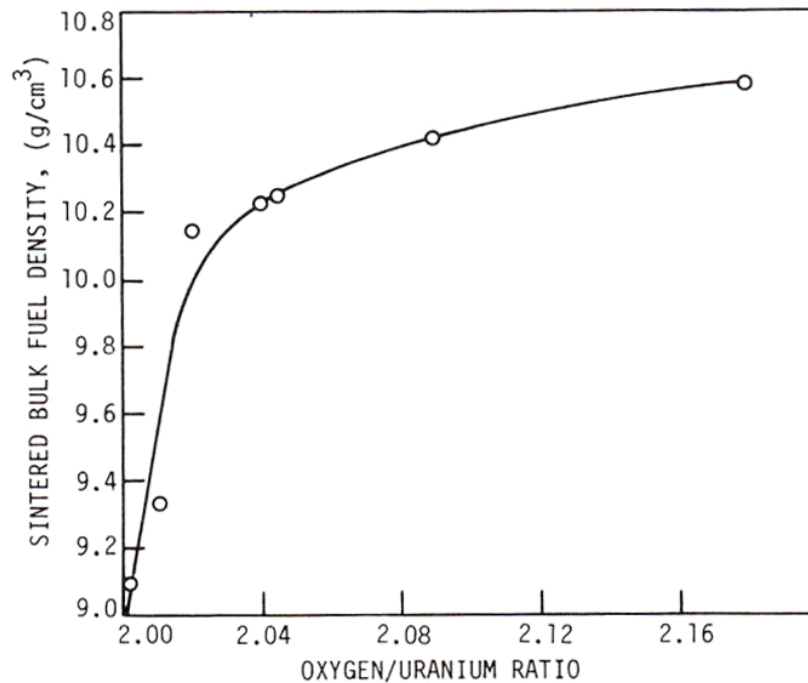


Figure 2. Bulk fuel density vs. oxygen content for uranium oxides sintered at 1450°C for 2 hours in argon.^{3,18}

From Figure 2, it follows that acceptable values of the sintered bulk UO_2 fuel density (around 9g/cm^3) can be achieved with very insignificant deviations from the stoichiometric composition, around $\text{UO}_{2.01}$. This does not affect its melting temperature and thermo-mechanical properties in a detrimental way. Consequently, the level of creep rate will remain almost the same as for the stoichiometric compound UO_2 (see Figure 4), while thermal conductivity – a property that is very sensitive to deviations from stoichiometry – will also be sufficiently close to that of the UO_2 (see Figure 3).

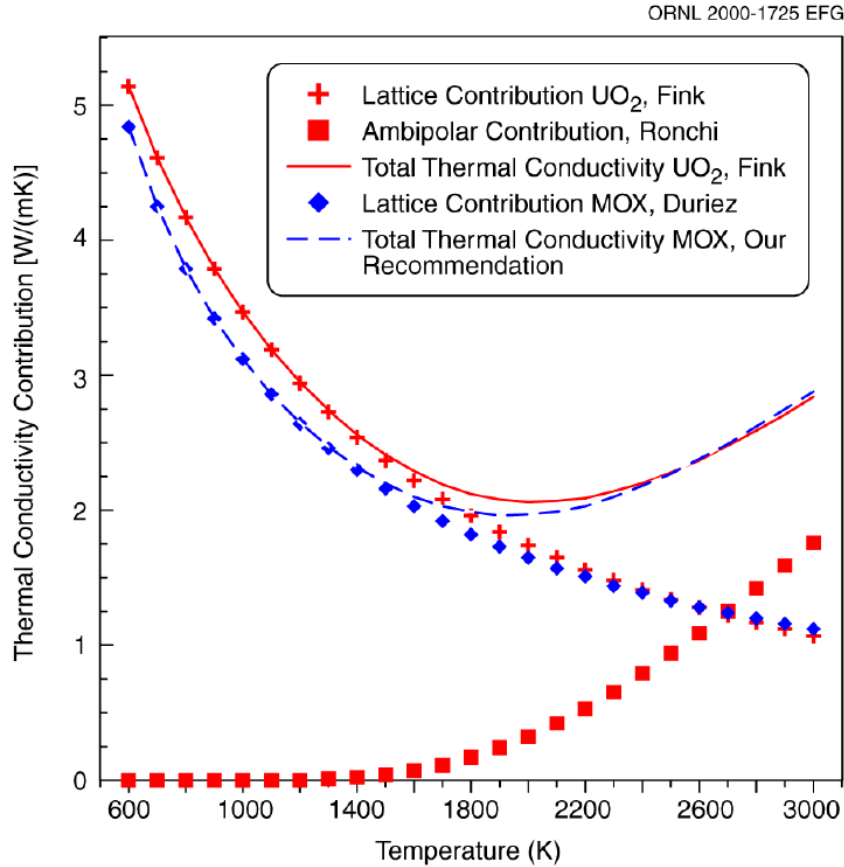


Figure 3. Variation of total thermal conductivity as a function of temperature and linear thermal expansion coefficient of UO_2 with temperature.⁷

Thermal conductivity of UO_2 is generally better for cast, rather than cold-pressed, material. Also, thermal conductivity increases with the increased density of compacted UO_2 .⁴ Generally, thermal conductivity varies quite substantially with deviations from UO_2 stoichiometry (lower at elevated temperatures [above 600°C] for hyper-stoichiometric materials [e.g., $\text{UO}_{2.01}$] and higher for hypo-stoichiometric materials [e.g., $\text{UO}_{1.97}$]).⁴ The comparison of thermal conductivities of UO_2 and U_3O_8 can be found below, in much greater detail.

Irradiation swelling in UO_2 will obviously depend upon the fuel burn-up and the temperature of the process. Finally, creep rate will be higher in the case of higher irradiation than for normal conditions (see Figure 4).

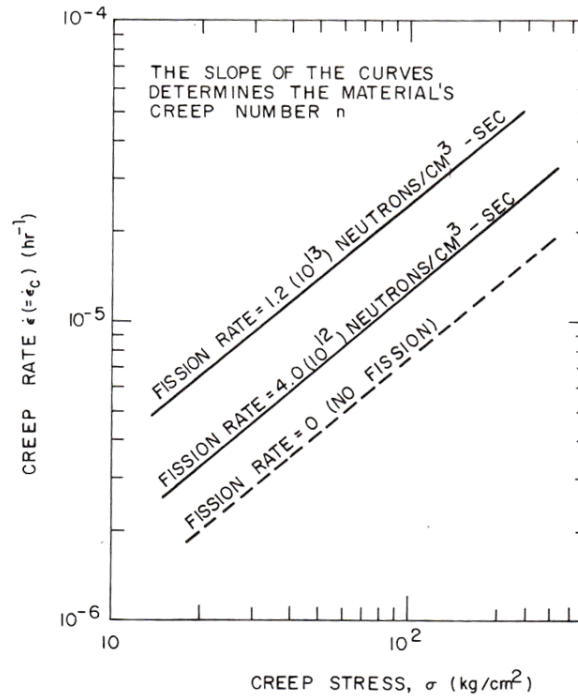


Figure 4. Variation of the UO_2 creep rate with and without irradiation.^{3,4}

2. THERMODYNAMICS AND KINETICS OF URANIUM OXIDES

Susceptibility of UO_2 to oxidation depends upon the average particle size.⁸ In very fine particles, UO_2 becomes easily oxidized to U_3O_8 in the presence of oxygen gas. However, when particles of UO_2 are at least $0.3\mu\text{m}$ large, UO_2 is fairly resistant to oxidation.⁸ Very dense, sintered UO_2 pellets will not get oxidized for many years as they are protected by the slightly oxidized thin surface film that is formed on large UO_2 grains.⁸ In any case, the UO_2 -based fuel must operate at as low external pressure as possible^a. The influence of external pressure upon the value of the Gibbs free energy change for the $3\text{UO}_2 + \text{O}_2 = \text{U}_3\text{O}_8$ (see Table 2).

^a See discussion below about pressure-dependent chemical interactions of UO_2 and the graphite matrix.

Table 2. Gibbs free energy for the reaction $3\text{UO}_2 + \text{O}_2 = \text{U}_3\text{O}_8$ as a function of temperature at pressure $P=0.05$ mbar, corresponding to the optimal conditions determined at ANL.⁹

```

Reaction: 302U1+02=08U3
02U1 stable as 02U1_$
02 stable as GAS
08U3 stable as 08U3_$

```

T (K)	Delta-Cp (Joule/K)	Delta-H (Joule)	Delta-S (Joule/K)	Delta-G (Joule)
298.15	1.87968E+01	-3.19800E+05	-2.49411E+02	-2.45438E+05
300.00	1.88529E+01	-3.19765E+05	-2.49295E+02	-2.44977E+05
400.00	1.97316E+01	-3.17808E+05	-2.43671E+02	-2.20340E+05
483.	---- 08U3 becomes 08U3_\$2 ,delta-H = 135.00			
500.00	1.87659E+01	-3.15742E+05	-2.39078E+02	-1.96203E+05
567.	---- 08U3 becomes 08U3_\$3 ,delta-H = 148.00			
600.00	1.74505E+01	-3.13783E+05	-2.35512E+02	-1.72476E+05
700.00	1.62976E+01	-3.12098E+05	-2.32912E+02	-1.49060E+05
800.00	1.55204E+01	-3.10511E+05	-2.30791E+02	-1.25878E+05
830.	---- 08U3 becomes 08U3_\$4 ,delta-H = 314.00			
900.00	1.48395E+01	-3.08680E+05	-2.28626E+02	-1.02917E+05
1000.00	1.42997E+01	-3.07224E+05	-2.27091E+02	-8.01327E+04
1100.00	1.38184E+01	-3.05818E+05	-2.25751E+02	-5.74921E+04
1200.00	1.33741E+01	-3.04459E+05	-2.24568E+02	-3.49773E+04
1300.00	1.29532E+01	-3.03142E+05	-2.23514E+02	-1.25742E+04
1400.00	1.25484E+01	-3.01868E+05	-2.22569E+02	9.72909E+03
1500.00	1.17131E+01	-3.00656E+05	-2.21733E+02	3.19432E+04
1600.00	1.06624E+01	-2.99532E+05	-2.21007E+02	5.40792E+04
1700.00	8.80847E+00	-2.98550E+05	-2.20411E+02	7.61489E+04
1800.00	5.72213E+00	-2.97812E+05	-2.19988E+02	9.81672E+04
1900.00	1.08408E+00	-2.97457E+05	-2.19796E+02	1.20154E+05
Temperature range exceeded for 08U3				

It is clear that this reaction becomes thermodynamically prohibited at temperatures slightly higher than 1000°C ($\Delta G > 0$).

On the other hand, at ambient pressure this phase reaction is allowed thermodynamically in all the range of temperatures considered above (see Table 3).

Table 3. Values of Gibbs free energy for the reaction $3\text{UO}_2 + \text{O}_2 = \text{U}_3\text{O}_8$ as a function of temperature at ambient pressure $P = 1013.25$ mbar (or ~ 1 atm). This Table also illustrates polymorphic transformations that take place at 210°C for $s1 \rightarrow s2$; at 397°C for $s2 \rightarrow s3$; and at 557°C for $s3 \rightarrow s4$ (our calculations).

```

Reaction: 3O2U1+O2=O8U3
O2U1 stable as O2U1_S
O2 stable as GAS
O8U3 stable as O8U3_S

```

T (K)	Delta-Cp (Joule/K)	Delta-H (Joule)	Delta-S (Joule/K)	Delta-G (Joule)
298.15	1.87968E+01	-3.19800E+05	-1.53687E+02	-2.73978E+05
300.00	1.88529E+01	-3.19765E+05	-1.53571E+02	-2.73694E+05
400.00	1.97316E+01	-3.17808E+05	-1.47947E+02	-2.58630E+05
483.	---- O8U3 becomes O8U3_S2 ,delta-H = 135.00			
500.00	1.87659E+01	-3.15742E+05	-1.43353E+02	-2.44065E+05
567.	---- O8U3 becomes O8U3_S3 ,delta-H = 148.00			
600.00	1.74505E+01	-3.13783E+05	-1.39787E+02	-2.29911E+05
700.00	1.62976E+01	-3.12098E+05	-1.37188E+02	-2.16067E+05
800.00	1.55204E+01	-3.10511E+05	-1.35067E+02	-2.02457E+05
830.	---- O8U3 becomes O8U3_S4 ,delta-H = 314.00			
900.00	1.48395E+01	-3.08680E+05	-1.32901E+02	-1.89069E+05
1000.00	1.42997E+01	-3.07224E+05	-1.31366E+02	-1.75857E+05
1100.00	1.38184E+01	-3.05818E+05	-1.30027E+02	-1.62789E+05
1200.00	1.33741E+01	-3.04459E+05	-1.28843E+02	-1.49847E+05
1300.00	1.29532E+01	-3.03142E+05	-1.27790E+02	-1.37016E+05
1400.00	1.25484E+01	-3.01868E+05	-1.26845E+02	-1.24285E+05
1500.00	1.17131E+01	-3.00656E+05	-1.26008E+02	-1.11643E+05
1600.00	1.06624E+01	-2.99532E+05	-1.25283E+02	-9.90797E+04
1700.00	8.80847E+00	-2.98550E+05	-1.24687E+02	-8.65824E+04
1800.00	5.72213E+00	-2.97812E+05	-1.24264E+02	-7.41366E+04
1900.00	1.08408E+00	-2.97457E+05	-1.24071E+02	-6.17220E+04
Temperature range exceeded for O8U3				

This requirement is particularly important for the TREAT reactor because the quality of vacuum inside the assembly affects heat transfer through the fuel-to-cladding gap in a profound way (see Reference 8). Consequently, a conclusion was made in the Argonne National Laboratory (ANL) study⁹ that pressure in the gap should be no higher than 0.05 mBar, which can be considered a perfect vacuum for thermal calculations. All calculations were made using the TAB module of ThermoCalc v.2015a and the SSUB4 database for thermodynamic properties of individual substances.¹⁰

UO_2 does not have any polymorphs (crystalline modifications), while U_3O_8 , according to the literature data,^{10,11} has four polymorphs (sometimes denoted as $s1$, $s2$, $s3$, and $s4$; see Tables 2 and 3 above⁸), of which only two are stable in normal conditions.¹¹ These polymorphic modifications of U_3O_8 are called “ α ” and “ β ”.¹² As pointed out above, the most stable α -modification possesses orthorhombic crystalline structure, while the β -modification – hexagonal.¹⁰ They are related but not identical in terms of their respective crystalline structures. Indeed, in the β - U_3O_8 structure, the uranium atoms are located in a single 3-fold position, while in the α - U_3O_8 , they occupy two types of positions: 2-fold and 4-fold. One can hypothesize that, in the case of a reactivity-initiated accident (RIA) or loss-of-coolant accident (LOCA), significant temperature excursions may result in the corresponding phase transformation, possibly accompanied by the loss of geometrical/structural stability of fuel rods.

The uranium-oxygen phase diagrams described in the literature do not yield a coherent picture. Indeed, depending upon the type of report (experimental vs computational) and the date of its publication, one can state that there is still no consensus about the number and stoichiometry of intermediate phases present in the system.^{13,14,15,16,17} Such phases as UO (in thin films⁴), UO₂, U₃O₈, UO₃, U₄O₉, U₃O₇, plus different non-stoichiometric compositions of the UO_{2±δ} have been reported. U₂O₅, U₁₃O₃₄, and U₅O₁₂ were noted in one reference (phase diagram),³ as well as U₈O_{21±x}.¹⁶ In the latter case, it was pointed out that the U₈O_{21±x} oxide produces metastable states that depend on sample morphology.¹⁶ Since these phases (U₂O₅, U₁₃O₃₄; U₅O₁₂; U₈O_{21±x}) were reported to be stable only at relatively low temperatures or in certain specific morphologies, we do not consider them here.

Of particular interest is the fact that the melting temperature of stoichiometric UO₂ (around 2865°C) decreases quite substantially when the O/U ratio is 1.68 (2425°C), and also when O/U ratio is 2.25 (2500°C), i.e., for both hypo- and hyper-stoichiometric compositions.¹² In turn, as pointed out above, both types of deviations from stoichiometry, quite unexpectedly, result in the undesired increase in the creep rate, sintering, diffusion and other properties dependent upon interatomic mobility.¹⁸

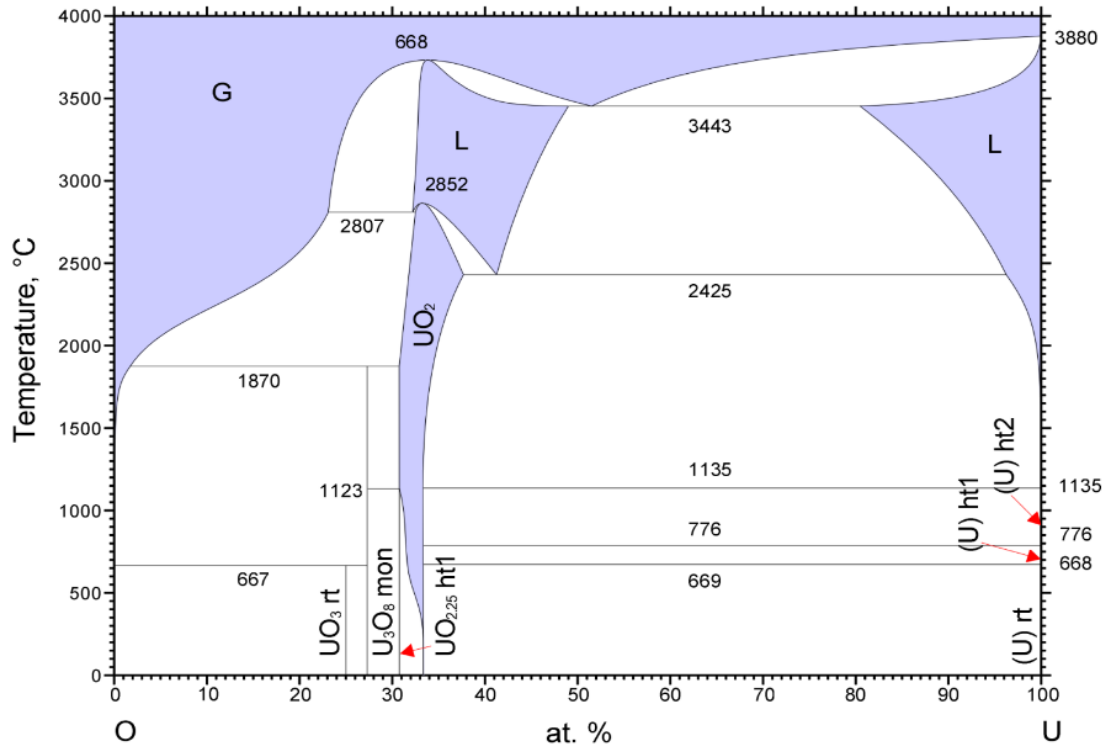


Figure 5. The calculated U-O phase diagram.¹³

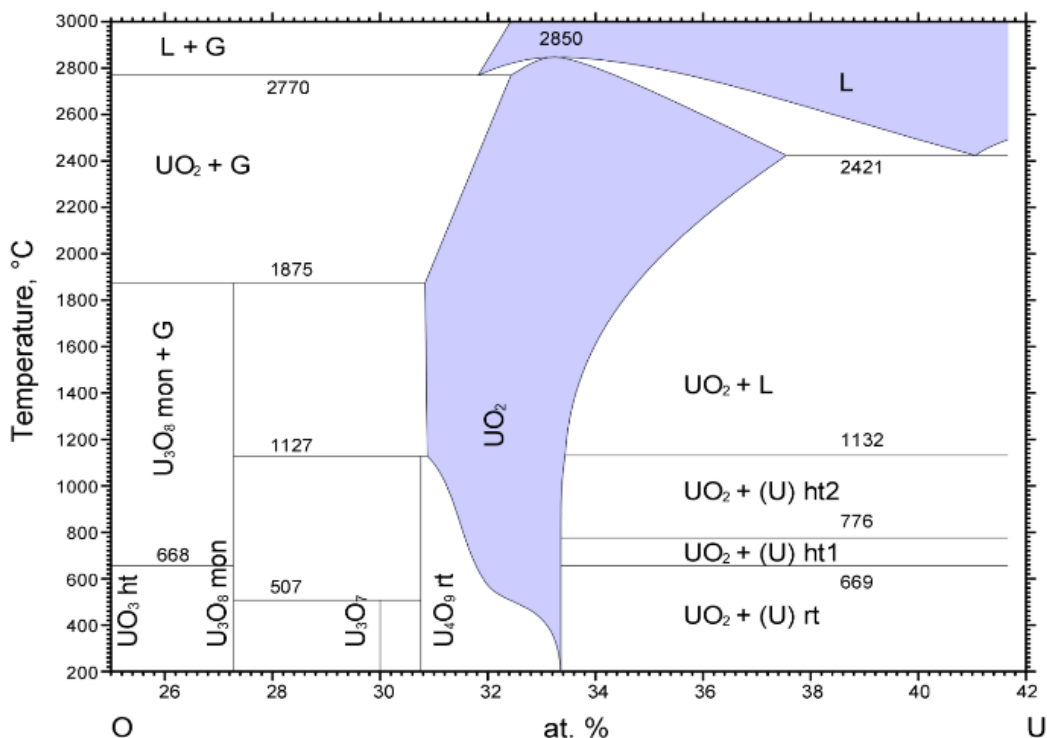


Figure 6. The U-O phase diagram according to Reference 14, calculated.

The two sources^{13,14} differ quite substantially in the phase compositions at low temperatures. This is not surprising, given that it is difficult to achieve equilibrium at such low temperatures as 200°C to 600°C in experimental studies. However, they are consistent in providing the melting temperature of UO_2 at 2850-2852°C. In both diagrams, UO_2 melts congruently. The existence of the several polytypes of U_3O_8 is also an established fact, as well as that of UO_3 and U_4O_9 (denoted sometimes as $\text{UO}_{2.25}$). The temperature of non-variant phase reaction $\text{U}_3\text{O}_8 \rightarrow \text{UO}_2 + \text{GAS}$ is also established reliably at ~ 1875°C (ambient pressure). (See Figure 5 and Figure 6.)

The terminal points of maximum and minimal solubility of oxygen in UO_2 are unambiguously determined as ~31 at.% U and ~38 at.% U, respectively, in both studies. The corresponding temperatures are defined by the non-variant phase transformation at 2425°C (maximum U solubility) and 1875°C (decomposition of U_3O_8 , minimum U solubility).

Therefore, one can say with confidence that all of the phase transformations related to the production and functioning of ceramic UO_2 -based nuclear fuel are very well established. Discrepancies are related only to the relatively low temperature regions of this phase diagram, which are considerably less important for the manufacturing and operation of nuclear fuel; see the phase diagram¹⁵ in Figure 7.

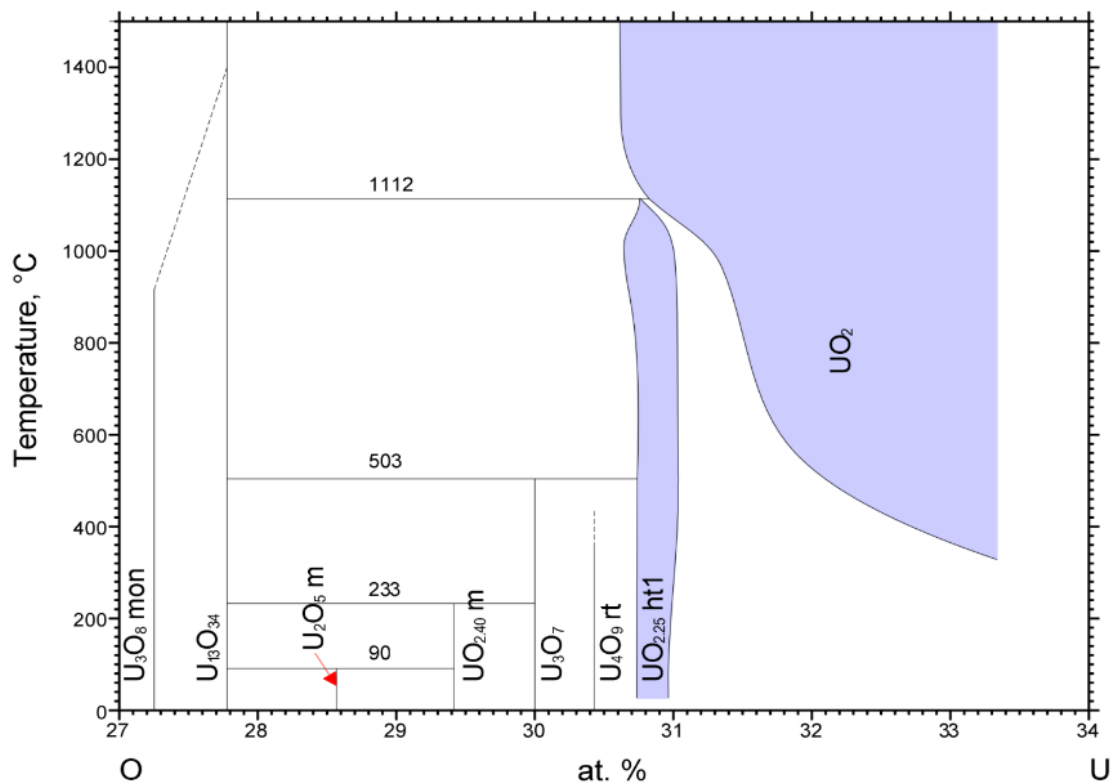


Figure 7. The U-O phase diagram constructed experimentally.¹⁵

A potential chemical interaction between nuclear fuel and the carbon (graphite) dispersion matrix is an important issue and is discussed below. Here, only the analysis of the isothermal cross-section of the U-O-C phase diagram was conducted (See Figure 8).¹⁶

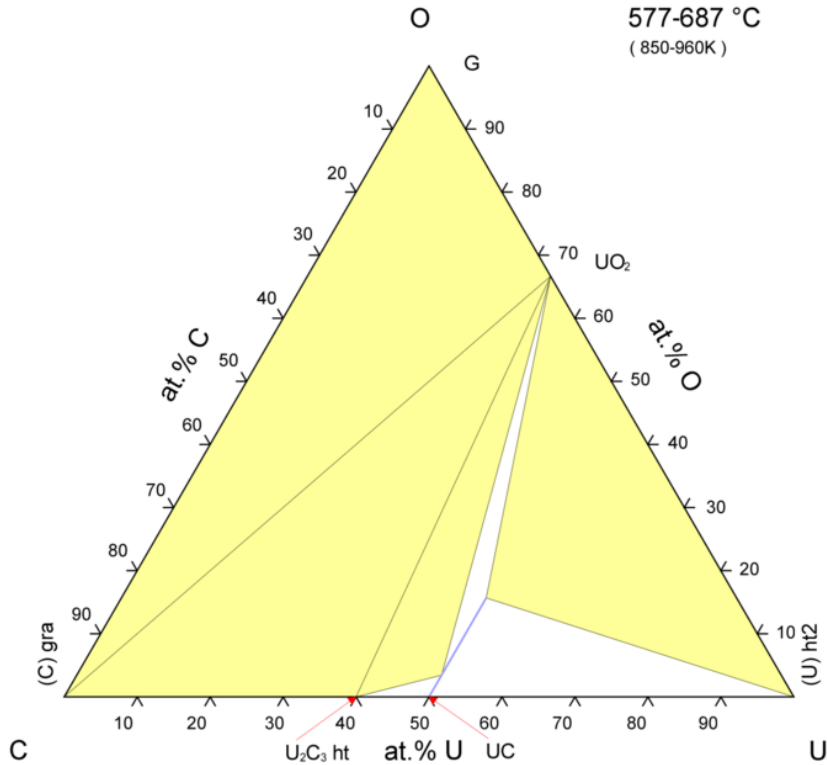


Figure 8. Isothermal cross-section of the U-C-O phase diagram.¹⁶

It is clear from this diagram that there is not any solubility of graphite in UO_2 , so a chemical reaction of UO_2 reduction with C is hardly feasible at the present conditions. There is some solubility of UO_2 in UC, but this effect is not relevant for the developed fuel for TREAT.

3. POTENTIAL INTERACTIONS INSIDE NUCLEAR FUEL (UO_2 AND U_3O_8 REACTING WITH GRAPHITE)

There is a “common belief” that, under certain conditions, at some point nuclear fuel, be it UO_2 or U_3O_8 , could chemically interact with the graphite matrix. Below, we address this issue in detail, considering a number of potential interactions and their feasibility, both at normal working conditions and at air ingress conditions.

3.1 Uranium Dioxide UO_2 vs U_3O_8 – General Considerations for Graphite Reactions

In UO_2 , uranium is tetravalent, while in U_3O_8 its degree of oxidation, at least formally, is 5.33. Therefore, U_3O_8 uranium is more oxidized than in UO_2 . Consequently, one could expect that, if any chemical interactions among uranium oxides and graphite are possible, U_3O_8 will get reduced by carbon in somewhat milder conditions than UO_2 . However, one has to consider the fact that UO_2 can easily form non-stoichiometric compounds of the $\text{UO}_{2\pm\delta}$, while ThO_2 and PuO_2 do not display such deviations from stoichiometry. These lattice instabilities invite additional scrutiny in terms of potential interactions with graphite. There is a clear need for calculating or revisiting the electronic structure of both oxides in order to understand the peculiarities of their oxidation behavior. For now, a number of such potential reactions are considered from a thermodynamic standpoint as follows

1. $\text{UO}_2 + \text{C} = 2\text{CO} + \text{U}$

For this reaction at ambient pressure, the temperature dependence of the Gibbs free energy of reaction upon temperature was considered (TAB module, Thermo-Calc 2015a).¹⁰ (See Table 4.)

Table 4. Gibbs free energy as a function of temperature for the reaction $\text{UO}_2 + \text{C} = 2\text{CO} + \text{U}$ at ambient pressure (101.325 kPa = 1013.25 mbar ~ 1MPa).

Reaction: 2C+02U1=U+2C101				
C stable as C_S				
02U1 stable as 02U1_S				
U stable as U_S				
C101 stable as GAS				

T (K)	Delta-Cp (Joule/K)	Delta-H (Joule)	Delta-S (Joule/K)	Delta-G (Joule)

298.15	5.27857E+00	8.63943E+05	3.57016E+02	7.57498E+05
300.00	5.00346E+00	8.63952E+05	3.57048E+02	7.56838E+05
400.00	-6.41905E+00	8.63831E+05	3.56779E+02	7.21120E+05
500.00	-1.29728E+01	8.62829E+05	3.54568E+02	6.85544E+05
600.00	-1.61500E+01	8.61349E+05	3.51879E+02	6.50221E+05
700.00	-1.68791E+01	8.59680E+05	3.49308E+02	6.15164E+05
800.00	-1.57507E+01	8.58035E+05	3.47110E+02	5.80347E+05
900.00	-1.34014E+01	8.56570E+05	3.45381E+02	5.45726E+05
942.	---- U becomes U_S2 ,delta-H = 2790.70			
1000.00	-1.82023E+01	8.57794E+05	3.46700E+02	5.11094E+05
1048.	---- U becomes U_S3 ,delta-H = 4757.20			
1100.00	-2.42894E+01	8.60420E+05	3.49211E+02	4.76288E+05
1200.00	-2.55899E+01	8.57925E+05	3.47041E+02	4.41477E+05
1300.00	-2.67930E+01	8.55306E+05	3.44944E+02	4.06878E+05
1400.00	-2.79311E+01	8.52569E+05	3.42917E+02	3.72485E+05
1408.	---- U becomes U_L ,delta-H = 9142.00			
1500.00	-1.87987E+01	8.59810E+05	3.48097E+02	3.37665E+05
1600.00	-2.00934E+01	8.57866E+05	3.46843E+02	3.02918E+05
1700.00	-2.16474E+01	8.55782E+05	3.45580E+02	2.68296E+05
1800.00	-2.36135E+01	8.53523E+05	3.44289E+02	2.33803E+05
1900.00	-2.61055E+01	8.51042E+05	3.42948E+02	1.99440E+05
2000.00	-2.94735E+01	8.48282E+05	3.41533E+02	1.65215E+05
2100.00	-3.34144E+01	8.45146E+05	3.40004E+02	1.31138E+05
2200.00	-3.84787E+01	8.41561E+05	3.38337E+02	9.72193E+04
2300.00	-4.47325E+01	8.37411E+05	3.36494E+02	6.34761E+04
2400.00	-5.23192E+01	8.32570E+05	3.34434E+02	2.99277E+04
2500.00	-6.13192E+01	8.26900E+05	3.32121E+02	-3.40234E+03
2600.00	-7.17976E+01	8.20257E+05	3.29517E+02	-3.64868E+04
2670.	---- 02U1 becomes 02U1_S2 ,delta-H = 1824.00			
2700.00	-9.68130E+01	8.10219E+05	3.25737E+02	-6.92717E+04
2773.00	-9.69016E+01	8.03149E+05	3.23154E+02	-9.29559E+04
TAB:				

We see that, for this hypothetical reaction to become allowed thermodynamically, the temperature in the system must be above 2400 K (~ 2123°C). However, metallic uranium will melt at 1408 K (~1135°C).

When external pressure is equal to 0.05 mbar (determined as maximal allowed or fuel elements at ANL), we get the results shown in Table 5.

Table 5. Values of Gibbs free energy for the reaction $\text{UO}_2 + \text{C} = 2\text{CO} + \text{U}$ as a function of temperature at external pressure of 0.05 mbar.

```

Reaction: 2C+02U1=U+2C101
C stable as C_$
02U1 stable as 02U1_$
U stable as U_$
C101 stable as GAS

```

T (K)	Delta-Cp (Joule/K)	Delta-H (Joule)	Delta-S (Joule/K)	Delta-G (Joule)
298.15	5.27857E+00	8.63943E+05	5.21701E+02	7.08397E+05
300.00	5.00346E+00	8.63952E+05	5.21733E+02	7.07432E+05
400.00	-6.41905E+00	8.63831E+05	5.21464E+02	6.55246E+05
500.00	-1.29728E+01	8.62829E+05	5.19254E+02	6.03202E+05
600.00	-1.61500E+01	8.61349E+05	5.16565E+02	5.51410E+05
700.00	-1.68791E+01	8.59680E+05	5.13993E+02	4.99884E+05
800.00	-1.57507E+01	8.58035E+05	5.11795E+02	4.48599E+05
900.00	-1.34014E+01	8.56570E+05	5.10067E+02	3.97510E+05
942.	---- U becomes U_\$2 ,delta-H = 2790.70			
1000.00	-1.82023E+01	8.57794E+05	5.11385E+02	3.46408E+05
1048.	---- U becomes U_\$3 ,delta-H = 4757.20			
1100.00	-2.42894E+01	8.60420E+05	5.13896E+02	2.95135E+05
1200.00	-2.55899E+01	8.57925E+05	5.11726E+02	2.43854E+05
1300.00	-2.67930E+01	8.55306E+05	5.09630E+02	1.92787E+05
1400.00	-2.79311E+01	8.52569E+05	5.07602E+02	1.41926E+05
1408.	---- U becomes U_\$L ,delta-H = 9142.00			
1500.00	-1.87987E+01	8.59810E+05	5.12782E+02	9.06368E+04
1600.00	-2.00934E+01	8.57866E+05	5.11528E+02	3.94213E+04
1700.00	-2.16474E+01	8.55782E+05	5.10265E+02	-1.16686E+04
1800.00	-2.36135E+01	8.53523E+05	5.08974E+02	-6.26309E+04
1900.00	-2.61055E+01	8.51042E+05	5.07634E+02	-1.13462E+05
2000.00	-2.94735E+01	8.48282E+05	5.06218E+02	-1.64155E+05
2100.00	-3.34144E+01	8.45146E+05	5.04689E+02	-2.14701E+05
2200.00	-3.84787E+01	8.41561E+05	5.03023E+02	-2.65088E+05
2300.00	-4.47325E+01	8.37411E+05	5.01179E+02	-3.15300E+05
2400.00	-5.23192E+01	8.32570E+05	4.99120E+02	-3.65317E+05
2500.00	-6.13192E+01	8.26900E+05	4.96806E+02	-4.15116E+05
2600.00	-7.17976E+01	8.20257E+05	4.94202E+02	-4.64669E+05
2670.	---- 02U1 becomes 02U1_\$2 ,delta-H = 1824.00			
2700.00	-9.68130E+01	8.10219E+05	4.90423E+02	-5.13922E+05
2773.00	-9.69016E+01	8.03149E+05	4.87839E+02	-5.49628E+05

At low pressure of 0.05 mbar, this reaction becomes thermodynamically possible at temperature somewhat above the metallic uranium melting point ($T_m = 1135^\circ\text{C}$), i.e., around $\sim 1450^\circ\text{C}$. In other words, this reaction is pressure sensitive but requires very deep reduction of uranium in the UO_2 to metallic uranium. From this perspective and considering our general thoughts above, the next reaction considered below is much more energetically favorable as pressure approaches zero and requires much more attention.

2. $\text{UO}_2 + 4\text{C} = \text{UC}_2 + 2\text{CO}$

For this reaction we get the following results at ambient pressure (see Table 6).

Table 6. Values of Gibbs free energy for the reaction $\text{UO}_2 + 4\text{C} = \text{UC}_2 + 2\text{CO}$ as a function of temperature at ambient pressure $P = 1013.25 \text{ mbar}$ (or $\sim 1 \text{ atm}$).

```

Reaction: 4C+02U1=C+2C101
C stable as C_S
02U1 stable as 02U1_S
C stable as C_S
C101 stable as GAS

```

T (K)	Delta-Cp (Joule/K)	Delta-H (Joule)	Delta-S (Joule/K)	Delta-G (Joule)
298.15	-3.09226E+01	8.63943E+05	3.01074E+02	7.74177E+05
300.00	-3.12891E+01	8.63885E+05	3.00882E+02	7.73621E+05
400.00	-4.79014E+01	8.59878E+05	2.89469E+02	7.44091E+05
500.00	-5.96238E+01	8.54467E+05	2.77443E+02	7.15746E+05
600.00	-6.77729E+01	8.48072E+05	2.65806E+02	6.88588E+05
700.00	-7.34255E+01	8.40995E+05	2.54908E+02	6.62559E+05
800.00	-7.73351E+01	8.33445E+05	2.44832E+02	6.37579E+05
900.00	-8.02607E+01	8.25560E+05	2.35549E+02	6.13566E+05
1000.00	-8.26913E+01	8.17409E+05	2.26963E+02	5.90446E+05
1100.00	-8.47694E+01	8.09034E+05	2.18982E+02	5.68154E+05
1200.00	-8.65961E+01	8.00464E+05	2.11526E+02	5.46632E+05
1300.00	-8.82433E+01	7.91720E+05	2.04529E+02	5.25833E+05
1400.00	-8.97627E+01	7.82819E+05	1.97933E+02	5.05713E+05
1500.00	-9.13391E+01	7.73763E+05	1.91685E+02	4.86235E+05
1600.00	-9.29279E+01	7.64551E+05	1.85740E+02	4.67366E+05
1700.00	-9.47453E+01	7.55170E+05	1.80054E+02	4.49078E+05
1800.00	-9.69501E+01	7.45589E+05	1.74578E+02	4.31348E+05
1900.00	-9.96607E+01	7.35763E+05	1.69266E+02	4.14157E+05
2000.00	-1.03231E+02	7.25637E+05	1.64073E+02	3.97491E+05
2100.00	-1.07360E+02	7.15116E+05	1.58940E+02	3.81341E+05
2200.00	-1.12601E+02	7.04128E+05	1.53830E+02	3.65702E+05
2300.00	-1.19021E+02	6.92557E+05	1.48687E+02	3.50576E+05
2400.00	-1.26767E+02	6.80279E+05	1.43463E+02	3.35968E+05
2500.00	-1.35918E+02	6.67157E+05	1.38108E+02	3.21888E+05
2600.00	-1.46542E+02	6.53047E+05	1.32575E+02	3.08352E+05
2670.	---- 02U1 becomes 02U1_S2 ,delta-H = 1824.00			
2700.00	-1.71698E+02	6.35527E+05	1.25972E+02	2.95403E+05
2773.00	-1.71886E+02	6.22986E+05	1.21389E+02	2.86375E+05

TAB: _

Consequently, this reaction is thermodynamically prohibited at any temperature of interest at ambient pressure.

Table 7. Values of Gibbs free energy for the reaction $\text{UO}_2 + 4\text{C} = \text{UC}_2 + 2\text{CO}$ as a function of temperature at ambient pressure $P = 0.05 \text{ mbar}$.

```

Reaction: 4C+02U1=C+2C101
C stable as C_$
02U1 stable as 02U1_$
C stable as C_$
C101 stable as GAS

```

T (K)	Delta-Cp (Joule/K)	Delta-H (Joule)	Delta-S (Joule/K)	Delta-G (Joule)
298.15	-3.09226E+01	8.63943E+05	4.65759E+02	7.25076E+05
300.00	-3.12891E+01	8.63885E+05	4.65567E+02	7.24215E+05
400.00	-4.79014E+01	8.59878E+05	4.54154E+02	6.78216E+05
500.00	-5.96238E+01	8.54467E+05	4.42128E+02	6.33403E+05
600.00	-6.77729E+01	8.48072E+05	4.30492E+02	5.89777E+05
700.00	-7.34255E+01	8.40995E+05	4.19593E+02	5.47280E+05
800.00	-7.73351E+01	8.33445E+05	4.09517E+02	5.05831E+05
900.00	-8.02607E+01	8.25560E+05	4.00234E+02	4.65350E+05
1000.00	-8.26913E+01	8.17409E+05	3.91648E+02	4.25761E+05
1100.00	-8.47694E+01	8.09034E+05	3.83667E+02	3.87000E+05
1200.00	-8.65961E+01	8.00464E+05	3.76211E+02	3.49010E+05
1300.00	-8.82433E+01	7.91720E+05	3.69214E+02	3.11742E+05
1400.00	-8.97627E+01	7.82819E+05	3.62618E+02	2.75154E+05
1500.00	-9.13391E+01	7.73763E+05	3.56371E+02	2.39207E+05
1600.00	-9.29279E+01	7.64551E+05	3.50426E+02	2.03870E+05
1700.00	-9.47453E+01	7.55170E+05	3.44739E+02	1.69113E+05
1800.00	-9.69501E+01	7.45589E+05	3.39263E+02	1.34915E+05
1900.00	-9.96607E+01	7.35763E+05	3.33951E+02	1.01255E+05
2000.00	-1.03231E+02	7.25637E+05	3.28758E+02	6.81207E+04
2100.00	-1.07360E+02	7.15116E+05	3.23626E+02	3.55019E+04
2200.00	-1.12601E+02	7.04128E+05	3.18515E+02	3.39482E+03
2300.00	-1.19021E+02	6.92557E+05	3.13373E+02	-2.82000E+04
2400.00	-1.26767E+02	6.80279E+05	3.08148E+02	-5.92770E+04
2500.00	-1.35918E+02	6.67157E+05	3.02793E+02	-8.98254E+04
2600.00	-1.46542E+02	6.53047E+05	2.97260E+02	-1.19830E+05
2670.	---- 02U1 becomes 02U1_\$2 ,delta-H = 1824.00			
2700.00	-1.71698E+02	6.35527E+05	2.90657E+02	-1.49247E+05
2773.00	-1.71886E+02	6.22986E+05	2.86074E+02	-1.70297E+05

So, when the pressure inside a fuel element becomes 0.05 mbar, this reaction becomes thermodynamically permissible around $\sim 2000^\circ\text{C}$ (See Table 7). Exploring a hypothetical case when $P = 0.01 \text{ mbar}$, we get different results as seen in Table 8.

Table 8. Values of Gibbs free energy for the reaction $\text{UO}_2 + 4\text{C} = \text{UC}_2 + 2\text{CO}$ as a function of temperature at $P=0.01$ mbar.

```

Reaction: 4C+02U1=C+2C101
C stable as C_$
02U1 stable as 02U1_$
C stable as C_$
C101 stable as GAS

```

T (K)	Delta-Cp (Joule/K)	Delta-H (Joule)	Delta-S (Joule/K)	Delta-G (Joule)
298.15	-3.09226E+01	8.63943E+05	4.92523E+02	7.17097E+05
300.00	-3.12891E+01	8.63885E+05	4.92330E+02	7.16186E+05
400.00	-4.79014E+01	8.59878E+05	4.80917E+02	6.67511E+05
500.00	-5.96238E+01	8.54467E+05	4.68891E+02	6.20021E+05
600.00	-6.77729E+01	8.48072E+05	4.57255E+02	5.73719E+05
700.00	-7.34255E+01	8.40995E+05	4.46357E+02	5.28545E+05
800.00	-7.73351E+01	8.33445E+05	4.36281E+02	4.84420E+05
900.00	-8.02607E+01	8.25560E+05	4.26997E+02	4.41263E+05
1000.00	-8.26913E+01	8.17409E+05	4.18412E+02	3.98998E+05
1100.00	-8.47694E+01	8.09034E+05	4.10430E+02	3.57560E+05
1200.00	-8.65961E+01	8.00464E+05	4.02975E+02	3.16894E+05
1300.00	-8.82433E+01	7.91720E+05	3.95977E+02	2.76950E+05
1400.00	-8.97627E+01	7.82819E+05	3.89381E+02	2.37685E+05
1500.00	-9.13391E+01	7.73763E+05	3.83134E+02	1.99062E+05
1600.00	-9.29279E+01	7.64551E+05	3.77189E+02	1.61048E+05
1700.00	-9.47453E+01	7.55170E+05	3.71502E+02	1.23616E+05
1800.00	-9.69501E+01	7.45589E+05	3.66027E+02	8.67408E+04
1900.00	-9.96607E+01	7.35763E+05	3.60715E+02	5.04050E+04
2000.00	-1.03231E+02	7.25637E+05	3.55521E+02	1.45939E+04
2100.00	-1.07360E+02	7.15116E+05	3.50389E+02	-2.07012E+04
2200.00	-1.12601E+02	7.04128E+05	3.45278E+02	-5.54846E+04
2300.00	-1.19021E+02	6.92557E+05	3.40136E+02	-8.97558E+04
2400.00	-1.26767E+02	6.80279E+05	3.34912E+02	-1.23509E+05
2500.00	-1.35918E+02	6.67157E+05	3.29556E+02	-1.56734E+05
2600.00	-1.46542E+02	6.53047E+05	3.24023E+02	-1.89414E+05
2670.	---- 02U1 becomes 02U1_\$2 ,delta-H = 1824.00			
2700.00	-1.71698E+02	6.35527E+05	3.17420E+02	-2.21508E+05
2773.00	-1.71886E+02	6.22986E+05	3.12837E+02	-2.44512E+05

In this case, the studied reaction becomes thermodynamically permissible already at $\sim 1800^\circ\text{C}$.

Finally, considering a hypothetical case when $P=0$, we get results as shown in Table 9.

Table 9. Values of Gibbs free energy for the reaction $\text{UO}_2 + 4\text{C} = \text{UC}_2 + 2\text{CO}$ as a function of temperature at P=0.

Reaction: 4C+02U1=C+2C101				
C stable as C_S				
02U1 stable as 02U1_S				
C stable as C_S				
C101 stable as GAS				

T (K)	Delta-Cp (Joule/K)	Delta-H (Joule)	Delta-S (Joule/K)	Delta-G (Joule)

298.15	-3.09226E+01	8.63943E+05	1.64121E+03	3.74614E+05
300.00	-3.12891E+01	8.63885E+05	1.64102E+03	3.71578E+05
400.00	-4.79014E+01	8.59878E+05	1.62961E+03	2.08034E+05
500.00	-5.96238E+01	8.54467E+05	1.61758E+03	4.56752E+04
600.00	-6.77729E+01	8.48072E+05	1.60595E+03	-1.15496E+05
700.00	-7.34255E+01	8.40995E+05	1.59505E+03	-2.75539E+05
800.00	-7.73351E+01	8.33445E+05	1.58497E+03	-4.34533E+05
900.00	-8.02607E+01	8.25560E+05	1.57569E+03	-5.92560E+05
1000.00	-8.26913E+01	8.17409E+05	1.56710E+03	-7.49694E+05
1100.00	-8.47694E+01	8.09034E+05	1.55912E+03	-9.06001E+05
1200.00	-8.65961E+01	8.00464E+05	1.55167E+03	-1.06154E+06
1300.00	-8.82433E+01	7.91720E+05	1.54467E+03	-1.21635E+06
1400.00	-8.97627E+01	7.82819E+05	1.53807E+03	-1.37048E+06
1500.00	-9.13391E+01	7.73763E+05	1.53183E+03	-1.52398E+06
1600.00	-9.29279E+01	7.64551E+05	1.52588E+03	-1.67686E+06
1700.00	-9.47453E+01	7.55170E+05	1.52019E+03	-1.82916E+06
1800.00	-9.69501E+01	7.45589E+05	1.51472E+03	-1.98090E+06
1900.00	-9.96607E+01	7.35763E+05	1.50941E+03	-2.13211E+06
2000.00	-1.03231E+02	7.25637E+05	1.50421E+03	-2.28279E+06
2100.00	-1.07360E+02	7.15116E+05	1.49908E+03	-2.43295E+06
2200.00	-1.12601E+02	7.04128E+05	1.49397E+03	-2.58261E+06
2300.00	-1.19021E+02	6.92557E+05	1.48883E+03	-2.73175E+06
2400.00	-1.26767E+02	6.80279E+05	1.48360E+03	-2.88037E+06
2500.00	-1.35918E+02	6.67157E+05	1.47825E+03	-3.02846E+06
2600.00	-1.46542E+02	6.53047E+05	1.47272E+03	-3.17601E+06
2670.	---- 02U1 becomes 02U1_S2 ,delta-H = 1824.00			
2700.00	-1.71698E+02	6.35527E+05	1.46611E+03	-3.32298E+06
2773.00	-1.71886E+02	6.22986E+05	1.46153E+03	-3.42983E+06

Therefore, the studied reaction becomes thermodynamically permissible at the relatively low temperature of ~300°C.

The obtained results somewhat substantiate a “popular belief” that this reaction is “possible” under certain conditions¹⁷: “Uranium dioxide is carbonized in contact with carbon, forming uranium carbide and carbon monoxide: $\text{UO}_2 + 4\text{C} \rightarrow \text{UC}_2 + 2\text{CO}$ This process must be done under an inert gas as uranium carbide is easily oxidized back into uranium oxide.”

This implies the need to select the maximum and minimum pressure and the gas or vacuum pressure inside the fuel / cladding gap very carefully and not only upon the considerations of heat transfer, but also taking into account the facts about chemical interaction as stated above.

3. $\text{U}_3\text{O}_8 + 8\text{C} = 3\text{U} + 8\text{CO}$

For this reaction, at ambient pressure we get results as shown in Table 10.

Table 10. Values of Gibbs free energy for the reaction $\text{U}_3\text{O}_8 + 8\text{C} = 3\text{U} + 8\text{CO}$ as a function of temperature at ambient pressure $P = 1013.25$ mbar (or ~ 1 atm).

```

Reaction: 8C+08U3=3U+8C101
C stable as C_$
08U3 stable as 08U3_$
U stable as U_$
C101 stable as GAS

```

T (K)	Delta-Cp (Joule/K)	Delta-H (Joule)	Delta-S (Joule/K)	Delta-G (Joule)
298.15	8.87274E+00	2.69057E+06	1.40343E+03	2.27214E+06
300.00	7.86747E+00	2.69059E+06	1.40349E+03	2.26954E+06
400.00	-3.40611E+01	2.68910E+06	1.39949E+03	2.12930E+06
483.	---- 08U3 becomes 08U3_S2 ,delta-H = 135.00			
500.00	-5.84572E+01	2.68422E+06	1.38872E+03	1.98985E+06
567.	---- 08U3 becomes 08U3_S3 ,delta-H = 148.00			
600.00	-7.08060E+01	2.67752E+06	1.37656E+03	1.85159E+06
700.00	-7.46552E+01	2.67019E+06	1.36526E+03	1.71450E+06
800.00	-7.22962E+01	2.66280E+06	1.35539E+03	1.57848E+06
830.	---- 08U3 becomes 08U3_S4 ,delta-H = 314.00			
900.00	-6.57346E+01	2.65556E+06	1.34685E+03	1.44340E+06
942.	---- U becomes U_S2 ,delta-H = 2790.70			
1000.00	-8.04542E+01	2.65666E+06	1.34810E+03	1.30856E+06
1048.	---- U becomes U_S3 ,delta-H = 4757.20			
1100.00	-9.89024E+01	2.66194E+06	1.35315E+03	1.17347E+06
1200.00	-1.02895E+02	2.65185E+06	1.34437E+03	1.03860E+06
1300.00	-1.06527E+02	2.64138E+06	1.33599E+03	9.04586E+05
1400.00	-1.09917E+02	2.63055E+06	1.32797E+03	7.71391E+05
1408.	---- U becomes U_L ,delta-H = 9142.00			
1500.00	-8.20244E+01	2.64969E+06	1.34173E+03	6.37097E+05
1600.00	-8.51744E+01	2.64133E+06	1.33633E+03	5.03195E+05
1700.00	-8.82879E+01	2.63266E+06	1.33108E+03	3.69826E+05
1800.00	-9.14036E+01	2.62367E+06	1.32594E+03	2.36976E+05
1900.00	-9.45517E+01	2.61437E+06	1.32092E+03	1.04634E+05
Temperature range exceeded for 08U3				

At pressure equal to $P = 0.05$ mbar, results were obtained as shown in Table 11.

Table 11. Values of Gibbs free energy for the reaction $\text{U}_3\text{O}_8 + 8\text{C} = 3\text{U} + 8\text{CO}$ at $P=0.05$ mbar.

Reaction: 8C+08U3=3U+8C101				
C stable as C_S				
08U3 stable as 08U3_S				
U stable as U_S				
C101 stable as GAS				
XX				
T	Delta-Cp	Delta-H	Delta-S	Delta-G
(K)	(Joule/K)	(Joule)	(Joule/K)	(Joule)
XX				
298.15	8.87274E+00	2.69057E+06	2.06218E+03	2.07573E+06
300.00	7.86747E+00	2.69059E+06	2.06223E+03	2.07192E+06
400.00	-3.40611E+01	2.68910E+06	2.05823E+03	1.86580E+06
483.	---- 08U3 becomes 08U3_S2 ,delta-H = 135.00			
500.00	-5.84572E+01	2.68422E+06	2.04746E+03	1.66048E+06
567.	---- 08U3 becomes 08U3_S3 ,delta-H = 148.00			
600.00	-7.08060E+01	2.67752E+06	2.03530E+03	1.45634E+06
700.00	-7.46552E+01	2.67019E+06	2.02401E+03	1.25339E+06
800.00	-7.22962E+01	2.66280E+06	2.01413E+03	1.05149E+06
830.	---- 08U3 becomes 08U3_S4 ,delta-H = 314.00			
900.00	-6.57346E+01	2.65556E+06	2.00559E+03	8.50528E+05
942.	---- U becomes U_S2 ,delta-H = 2790.70			
1000.00	-8.04542E+01	2.65666E+06	2.00684E+03	6.49823E+05
1048.	---- U becomes U_S3 ,delta-H = 4757.20			
1100.00	-9.89024E+01	2.66194E+06	2.01190E+03	4.48859E+05
1200.00	-1.02895E+02	2.65185E+06	2.00312E+03	2.48112E+05
1300.00	-1.06527E+02	2.64138E+06	1.99473E+03	4.82226E+04
1400.00	-1.09917E+02	2.63055E+06	1.98671E+03	-1.50847E+05
1408.	---- U becomes U_L ,delta-H = 9142.00			
1500.00	-8.20244E+01	2.64969E+06	2.00047E+03	-3.51015E+05
1600.00	-8.51744E+01	2.64133E+06	1.99507E+03	-5.50791E+05
1700.00	-8.82879E+01	2.63266E+06	1.98982E+03	-7.50034E+05
1800.00	-9.14036E+01	2.62367E+06	1.98468E+03	-9.48758E+05
1900.00	-9.45517E+01	2.61437E+06	1.97966E+03	-1.14697E+06
Temperature range exceeded for 08U3				

This reaction becomes possible at temperature around $\sim 1100^\circ\text{C}$.

4. $\text{U}_3\text{O}_8 + 14\text{C} = 3\text{UC}_2 + 8\text{CO}$

For this reaction, at ambient pressure we get results as shown in Table 12.

Table 12. Values of Gibbs free energy for the reaction $\text{U}_3\text{O}_8 + 8\text{C} = 3\text{U} + 8\text{CO}$ at P=1 atm.

```

Reaction: 14C+08U3=3C+8C101
C stable as C_$
08U3 stable as 08U3_$
C stable as C_$
C101 stable as GAS

```

T (K)	Delta-Cp (Joule/K)	Delta-H (Joule)	Delta-S (Joule/K)	Delta-G (Joule)
298.15	-9.97309E+01	2.69057E+06	1.23561E+03	2.32217E+06
300.00	-1.01010E+02	2.69038E+06	1.23499E+03	2.31989E+06
400.00	-1.58508E+02	2.67724E+06	1.19756E+03	2.19821E+06
483.	---- 08U3 becomes 08U3_\$2 ,delta-H = 135.00			
500.00	-1.98410E+02	2.65913E+06	1.15734E+03	2.08046E+06
567.	---- 08U3 becomes 08U3_\$3 ,delta-H = 148.00			
600.00	-2.25675E+02	2.63769E+06	1.11834E+03	1.96669E+06
700.00	-2.44294E+02	2.61413E+06	1.08206E+03	1.85669E+06
800.00	-2.57050E+02	2.58903E+06	1.04856E+03	1.75018E+06
830.	---- 08U3 becomes 08U3_\$4 ,delta-H = 314.00			
900.00	-2.66313E+02	2.56253E+06	1.01735E+03	1.64692E+06
1000.00	-2.73921E+02	2.53551E+06	9.88884E+02	1.54662E+06
1100.00	-2.80343E+02	2.50778E+06	9.62467E+02	1.44907E+06
1200.00	-2.85914E+02	2.47947E+06	9.37830E+02	1.35407E+06
1300.00	-2.90878E+02	2.45062E+06	9.14746E+02	1.26145E+06
1400.00	-2.95411E+02	2.42130E+06	8.93021E+02	1.17107E+06
1500.00	-2.99646E+02	2.39155E+06	8.72494E+02	1.08281E+06
1600.00	-3.03678E+02	2.36138E+06	8.53026E+02	9.96541E+05
1700.00	-3.07582E+02	2.33082E+06	8.34498E+02	9.12172E+05
1800.00	-3.11414E+02	2.29987E+06	8.16808E+02	8.29613E+05
1900.00	-3.15217E+02	2.26854E+06	7.99869E+02	7.48785E+05

Temperature range exceeded for 08U3

At P=1 atm this reaction is impossible in the whole range of studied temperatures.

When P=0.05 mbar, we get the following results in Table 13.

Table 13. Values of Gibbs free energy for the reaction $U_3O_8 + 8C = 3U + 8CO$ at P=0.05 mbar.

```

Reaction: 14C+08U3=3C+8C101
C stable as C_$
08U3 stable as 08U3_$
C stable as C_$
C101 stable as GAS
  
```

T (K)	Delta-Cp (Joule/K)	Delta-H (Joule)	Delta-S (Joule/K)	Delta-G (Joule)
298.15	-9.97309E+01	2.69057E+06	1.89435E+03	2.12577E+06
300.00	-1.01010E+02	2.69038E+06	1.89373E+03	2.12227E+06
400.00	-1.58508E+02	2.67724E+06	1.85630E+03	1.93472E+06
483.	---- 08U3 becomes 08U3_\$2 ,delta-H = 135.00			
500.00	-1.98410E+02	2.65913E+06	1.81609E+03	1.75109E+06
567.	---- 08U3 becomes 08U3_\$3 ,delta-H = 148.00			
600.00	-2.25675E+02	2.63769E+06	1.77708E+03	1.57144E+06
700.00	-2.44294E+02	2.61413E+06	1.74081E+03	1.39557E+06
800.00	-2.57050E+02	2.58903E+06	1.70730E+03	1.22319E+06
830.	---- 08U3 becomes 08U3_\$4 ,delta-H = 314.00			
900.00	-2.66313E+02	2.56253E+06	1.67609E+03	1.05405E+06
1000.00	-2.73921E+02	2.53551E+06	1.64763E+03	8.87881E+05
1100.00	-2.80343E+02	2.50778E+06	1.62121E+03	7.24455E+05
1200.00	-2.85914E+02	2.47947E+06	1.59657E+03	5.63580E+05
1300.00	-2.90878E+02	2.45062E+06	1.57349E+03	4.05089E+05
1400.00	-2.95411E+02	2.42130E+06	1.55176E+03	2.48837E+05
1500.00	-2.99646E+02	2.39155E+06	1.53124E+03	9.46966E+04
1600.00	-3.03678E+02	2.36138E+06	1.51177E+03	-5.74452E+04
1700.00	-3.07582E+02	2.33082E+06	1.49324E+03	-2.07688E+05
1800.00	-3.11414E+02	2.29987E+06	1.47555E+03	-3.56121E+05
1900.00	-3.15217E+02	2.26854E+06	1.45861E+03	-5.02823E+05
Temperature range exceeded for 08U3				

Therefore, at P=0.05 mbar, U_3O_8 can be reduced to UC_2 beginning at ~1300°C. Finally, for a hypothetical case when P=0, we get results as seen in Table 14.

Table 14. Values of Gibbs free energy for the reaction $\text{U}_3\text{O}_8 + 8\text{C} = 3\text{U} + 8\text{CO}$ at $P=0$.

Reaction: 14C+08U3=3C+8C101				
C stable as C_\$				
08U3 stable as 08U3_\$				
C stable as C_\$				
C101 stable as GAS				

T	Delta-Cp	Delta-H	Delta-S	Delta-G
(K)	(Joule/K)	(Joule)	(Joule/K)	(Joule)

298.15	-9.97309E+01	2.69057E+06	6.59617E+03	7.23922E+05
300.00	-1.01010E+02	2.69038E+06	6.59555E+03	7.11720E+05
400.00	-1.58508E+02	2.67724E+06	6.55812E+03	5.39881E+04
483.	---- 08U3 becomes 08U3_\$2 ,delta-H = 135.00			
500.00	-1.98410E+02	2.65913E+06	6.51791E+03	-5.99823E+05
567.	---- 08U3 becomes 08U3_\$3 ,delta-H = 148.00			
600.00	-2.25675E+02	2.63769E+06	6.47890E+03	-1.24965E+06
700.00	-2.44294E+02	2.61413E+06	6.44263E+03	-1.89570E+06
800.00	-2.57050E+02	2.58903E+06	6.40912E+03	-2.53827E+06
830.	---- 08U3 becomes 08U3_\$4 ,delta-H = 314.00			
900.00	-2.66313E+02	2.56253E+06	6.37791E+03	-3.17759E+06
1000.00	-2.73921E+02	2.53551E+06	6.34945E+03	-3.81394E+06
1100.00	-2.80343E+02	2.50778E+06	6.32303E+03	-4.44755E+06
1200.00	-2.85914E+02	2.47947E+06	6.29839E+03	-5.07861E+06
1300.00	-2.90878E+02	2.45062E+06	6.27531E+03	-5.70728E+06
1400.00	-2.95411E+02	2.42130E+06	6.25358E+03	-6.33371E+06
1500.00	-2.99646E+02	2.39155E+06	6.23306E+03	-6.95804E+06
1600.00	-3.03678E+02	2.36138E+06	6.21359E+03	-7.58036E+06
1700.00	-3.07582E+02	2.33082E+06	6.19506E+03	-8.20078E+06
1800.00	-3.11414E+02	2.29987E+06	6.17737E+03	-8.81940E+06
1900.00	-3.15217E+02	2.26854E+06	6.16043E+03	-9.43628E+06
Temperature range exceeded for 08U3				

Consequently, U_3O_8 becomes unstable with respect to reduction to UC_2 at a very low temperature of $\sim 200^\circ\text{C}$.

Summing up this section of the report, we can say that, in terms of chemical stability with respect to the process of reduction with carbon, both oxides exhibit unstable behavior at very low pressure. However, as expected, U_3O_8 is reduced more easily in the carbon matrix (i.e., at lower temperatures with all other conditions being equal) than UO_2 . Consequently, no advantages could be gained by utilizing the U_3O_8 -based fuel.

4. AIR INGRESS AND ITS INFLUENCE UPON UO_2 FUEL STOICHIOMETRY AND ZIRCONIUM-BASED CLADDING

In the unlikely event of air ingress, the fuel rods will be exposed to air-containing atmospheres at high temperatures. In comparison with steam, the presence of air is expected to result in a more rapid escalation of the accident. In particular, the presence of air can lead to the accelerated oxidation of the Zircaloy cladding, compared to that in steam, because of the faster kinetics, while the 85% higher heat of reaction will introduce the positive feedback loop and drive the process even further.²⁰

Previously, air ingress has been shown to cause poor heat transfer. In technical literature¹⁹ it is noted that the combined effect of these factors can give rise to an increased rate of fuel assembly degradation. In oxygen-starved conditions, nitriding of the metal can occur (this requires thermodynamic verification); the resulting zirconium nitride is highly inflammable.¹⁸ It can detonate on re-introduction of oxygen or steam, e.g., during core re-flood. Furthermore, the exposure of UO_2 to air at elevated temperatures can lead to increased release of some fission products, notably the highly-radiotoxic ruthenium,^{21,22} while the air is likely to further weaken the damaged cladding as a barrier against fission product release.

The mechanisms of oxygen stoichiometry variation in UO_2 at different temperature and oxygen partial pressure were studied using DFT (Reference 23). The authors emphasized that very limited experimental studies are available to understand the atomic structure of UO_2 near surface and defect effects of near surface on stoichiometry. By using their computational approach, the authors made a conclusion that, under the poor oxygen conditions, the stoichiometry is switched from hyper-stoichiometric at 300 K with a depth around 3 nm to near-stoichiometric at 1000 K and hypo-stoichiometric structure at 2000 K. Furthermore, at very poor oxygen concentrations and high temperatures, the results obtained by the authors also suggest that the bulk of the UO_2 is energetically more favorable to be hypo-stoichiometric, although the surface of OU_2 remains near-stoichiometric.²³

5. VOLUMETRIC CHANGES DURING FUEL BLOCK MANUFACTURING (950°C) AND DURING SUBSEQUENT OPERATION UP TO 820°C

Data on the thermal expansion characteristics of UO_2 is presented in Figure 9^{3,18}.

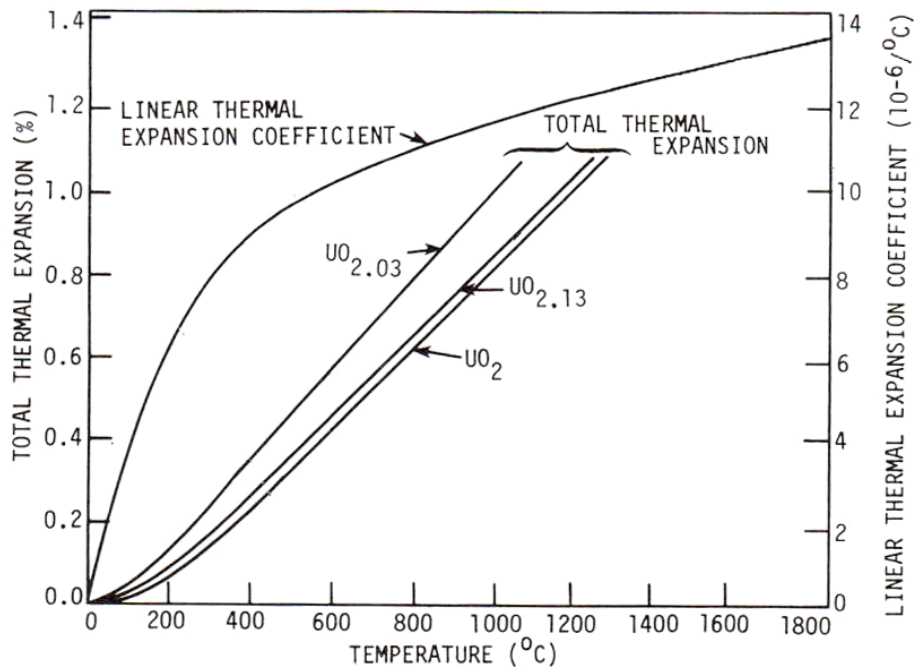


Figure 9. Variation of total thermal expansion and linear thermal expansion coefficient of UO_2 with temperature.^{3,18}

The coefficients of thermal expansion of the MOX fuel and stoichiometric $\text{UO}_{2.00}$ are presented in Table 15 below.

Table 15. Coefficients of thermal expansion of the MOX fuel and stoichiometric $\text{UO}_{2.00}$.²³

Temperature (K)	Relative thermal expansion $\Delta L(T)/L(273)$	Average linear thermal expansion coefficient (1/K)	TLTEC (1/K)	Density of $\text{UO}_{2.00}$ (kg/m^3)
3.0000E+02	2.6811E-04	9.9300E-06	9.7555E-06	1.0961E+04
4.0000E+02	1.2456E-03	9.8081E-06	9.7841E-06	1.0929E+04
5.0000E+02	2.2283E-03	9.8161E-06	9.8388E-06	1.0897E+04
6.0000E+02	3.2187E-03	9.8430E-06	9.9196E-06	1.0865E+04
7.0000E+02	4.2195E-03	9.8817E-06	1.0026E-05	1.0832E+04
8.0000E+02	5.2333E-03	9.9304E-06	1.0159E-05	1.0800E+04
9.0000E+02	6.2628E-03	9.9885E-06	1.0317E-05	1.0766E+04
1.0000E+03	7.3001E-03	1.0041E-05	1.0515E-05	1.0733E+04
1.1000E+03	8.3725E-03	1.0124E-05	1.0782E-05	1.0699E+04
1.2000E+03	9.4768E-03	1.0223E-05	1.1120E-05	1.0664E+04
1.3000E+03	1.0620E-02	1.0341E-05	1.1529E-05	1.0628E+04
1.4000E+03	1.1810E-02	1.0479E-05	1.2008E-05	1.0590E+04
1.5000E+03	1.3054E-02	1.0639E-05	1.2558E-05	1.0551E+04
1.6000E+03	1.4359E-02	1.0821E-05	1.3177E-05	1.0511E+04
1.7000E+03	1.5733E-02	1.1025E-05	1.3865E-05	1.0468E+04
1.8000E+03	1.7182E-02	1.1252E-05	1.4622E-05	1.0423E+04
1.9000E+03	1.8714E-02	1.1502E-05	1.5447E-05	1.0376E+04
2.0000E+03	2.0337E-02	1.1776E-05	1.6341E-05	1.0327E+04
2.1000E+03	2.2057E-02	1.2073E-05	1.7302E-05	1.0275E+04
2.2000E+03	2.3883E-02	1.2394E-05	1.8331E-05	1.0220E+04
2.3000E+03	2.5820E-02	1.2738E-05	1.9427E-05	1.0162E+04

In the range from 0°C and up to 650°C, the expressions recommended by Martin²⁴ should be used for the relative thermal expansion, the true linear expansion coefficient (TLTEC), and density of solid stoichiometric $\text{UO}_{2.00}$ or very similar MOX fuel²⁵:

$$\Delta L(T)/L(273) = -2.66 * 10^{-3} + 9.802 * 10^{-6} * T - 2.705 * 10^{-10} * T^2 + 4.391 * 10^{-13} * T^3 ;$$

$$L(T) = L(273) * (9.9734 * 10^{-1} + 9.802 * 10^{-6} * T - 2.705 * 10^{-10} * T^2 + 4.391 * 10^{-13} * T^3) ;$$

$$\alpha_s(T) = 9.828 * 10^{-6} - 6.39 * 10^{-1} * T + 1.33 * 10^{-12} * T^2 - 1.757 * 10^{-17} * T^3 , (1/K) ;$$

$$\rho_s(T) = \rho_s(273)$$

$$* (9.9734 * 10^{-1} + 9.802 * 10^{-6} * T - 2.705 * 10^{-10} * T^2 + 4.391 * 10^{-13} * T^3)^{-3} , (\text{kg/m}^3) ;$$

In the temperature range from 923K and up to the melting point of UO_2 , the regression equations are given as follows⁷:

$$\begin{aligned}\Delta L(T)/L(273) &= -3.28 * 10^{-3} + 1.179 * 10^{-5} * T - 2.429 * 10^{-9} * T^2 + 1.219 * 10^{-12} * T^3 ; \\ L(T) &= L(273) * (9.9672 * 10^{-1} + 1.179 * 10^{-5} * T - 2.429 * 10^{-9} * T^2 + 1.219 * 10^{-12} * T^3) ; \\ \alpha_s(T) &= 1.1833 * 10^{-5} - 5.013 * 10^{-9} * T + 3.756 * 10^{-12} * T^2 - 6.125 * 10^{-17} * T^3 , (1/K) ; \\ \rho_s(T) &= \rho_s(273) \\ &\quad * (9.9672 * 10^{-1} + 1.179 * 10^{-5} * T - 2.429 * 10^{-9} * T^2 + 1.219 * 10^{-12} * T^3)^{-3} , [\text{kg/m}^3]\end{aligned}$$

In the case of U_3O_8 , the situation with thermal expansion is somewhat more complex.²⁴ Detailed thermal expansion data for U_3O_8 have been obtained by high-temperature X-ray diffractometric data between 22°C and 1100°C.²⁵ It was established that stoichiometric U_3O_8 changes continuously, reversibly and anisotropically above room temperature with expansion along the a-axis and contraction along the b-axis from orthorhombic to hexagonal symmetry at 350°C ± 10°C.²⁵ A small but continuous contraction along the c-axis occurs up to 1100°C. The loss of oxygen begins around 600°C, but this does not result in any discontinuity in both parameters of the hexagonal phase (i.e., “a” and “c”) up to 875°C.

However, in the temperature range from 875°C to 925°C, the structure undergoes a change to lower symmetry as a result of contraction along the a-axis and expansion along the b-axis (expansion-contraction anomaly). This structural change is accompanied by a more extensive loss of oxygen and is usually irreversible unless the crystallite size is sufficiently small, ~0.05µm. On the other hand, during fuel block manufacturing, the temperature can reach as high as 950°C, while at normal conditions of fuel operation it is maintained at ~820°C.

Therefore, because of the anisotropic and some irreversible changes in the U_3O_8 crystalline structure and tendency to lose oxygen at temperature above 600°C, UO_2 shows significantly more thermal stability over the thermal stability of U_3O_8 . In addition, the thermo-physical properties of UO_2 are exceptionally well understood and display highly predictable behavior without any discontinuities and allotropic transformations. This should serve as yet another argument in favor of UO_2 rather than U_3O_8 , that can undergo polymorphic transformations.

6. OPTIMAL MANUFACTURING CONDITIONS

In this report, a number of factors were considered that might affect the chemical and dimensional stability of the TREAT nuclear fuel. Assuming that the UO_2 -carbon matrix fuel will be selected for the TREAT restart, one has to consider the optimal gas filling of the gap between the fuel and the Zry-4 cladding. Special attention was paid above to the two types of conditions existing at the same time in the fuel. On the one hand, the presence of even minor amounts of oxygen in the gap is highly undesirable because of the potential oxidation of carbon to CO or CO_2 at 820°C. Also, a possibility of the oxidative process resulting in the chemical reaction $\text{UO}_2 \rightarrow \text{U}_3\text{O}_8$ should be excluded. Consequently, the atmosphere in the gap should be that of an inert gas and the pressure – as recommended in the ANL study, i.e., 0.05 mbar or lower. It is assumed that inside the carbon- UO_2 fuel the particles of the UO_2 will be under the compressive stress, and, therefore, no reduction of UO_2 to UC_2 should be possible.

However, this second process is always a distinct possibility if the temperature in the system is sufficiently high, and, at least in parts of the composite fuel, pressure upon the UO_2 particles could be negligible. This second reaction should be explored further including the first-principles atomistic calculations under different stress field distribution in the composite.

7. THERMAL CONDUCTIVITY OF UO_2 AND U_3O_8

Thermo-physical properties of both oxides were studied quite extensively, especially for UO_2 .^{24,27,28} The summary thermal conductivity curve(s) as functions of temperature for UO_2 are presented in Figure 10.²²

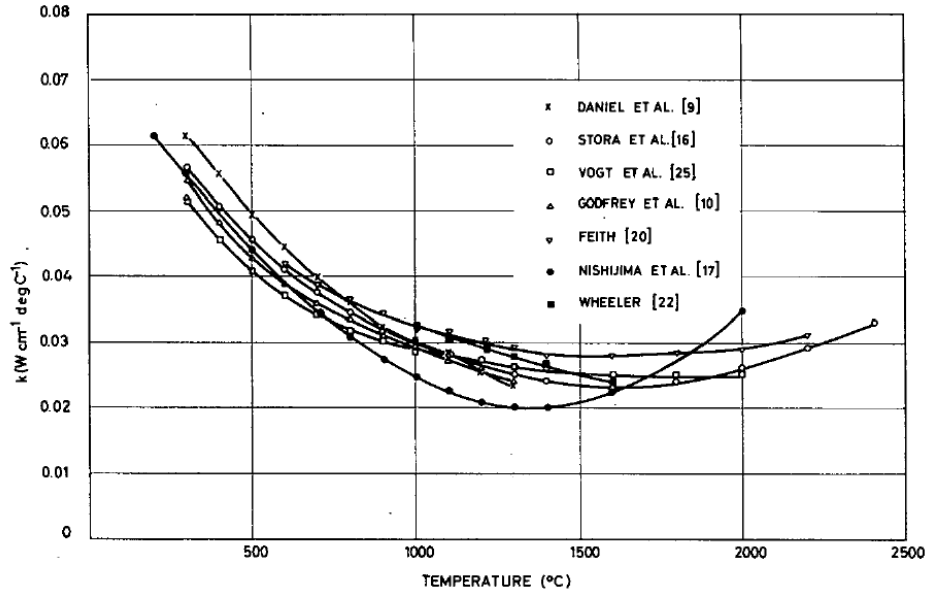


Figure 10. Thermal conductivity of un-irradiated polycrystalline $\text{UO}_{2.00}$.²⁴

The thermal conductivity of orthorhombic $\alpha\text{-U}_3\text{O}_8$ has been measured in air from 300 to 1100 K using an axial heat flow comparative set-up²³ (See Figure 11.) The results show that the conductivity decreases monotonically with increasing temperature. The observed conductivity can be explained in terms of the phonon-defects and phonon-phonon interaction processes.

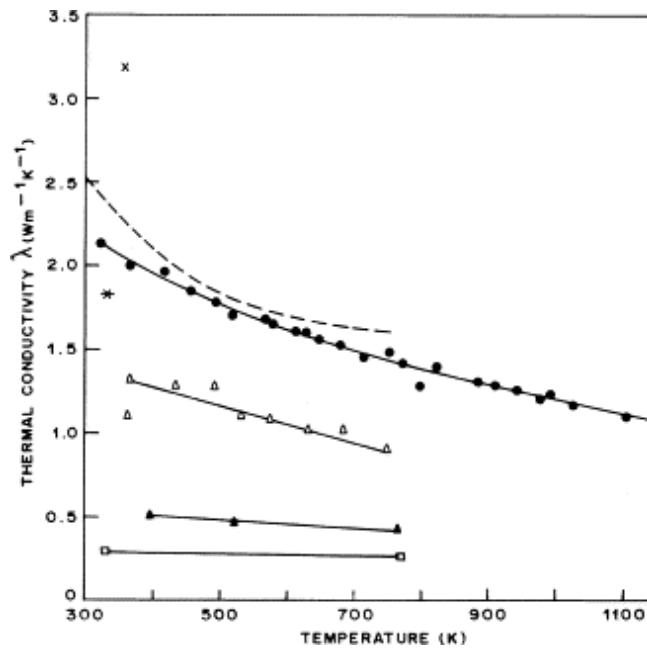


Figure 11. Thermal conductivity of U_3O_8 corrected to 100% theoretical density as a function of temperature according to different data; (●) present data.²⁷

Comparing the data for UO_2 and U_3O_8 , the thermal conductivity of UO_2 is almost one order of magnitude higher than that of U_3O_8 , although the exact ratio will be temperature-dependent. For both ceramic materials, as expected, the thermal conductivity values are low. Indeed, for comparison, the thermal conductivity of pure aluminum is $240 \text{ W} \cdot (\text{m}^{-1} \cdot \text{C}^{-1})$ at 100°C .⁵ As the neutron fluence (to which both materials were exposed) grows, thermal conductivity decreases for both oxides.²⁹

In the recent experimental work²⁹ it was established that for UO_2 , the thermal conductivity was $10.2 \text{ W/m} \cdot \text{K}$ at 323 K , and with increasing temperatures its behavior was inversely proportional to the temperature. At 648 K the thermal conductivity is $4.9 \text{ W/m} \cdot \text{K}$. The thermal conductivity peaks between 200 and 250 K and decreases for decreasing temperatures. Upon irradiation, the thermal conductivity at 323 K decreases to $8.6 \text{ W/m} \cdot \text{K}$ for a dose of $5 \times 10^{13} \text{ Ar}^+/\text{cm}^2$ and to $4 \text{ W/m} \cdot \text{K}$ for $7 \times 10^{14} \text{ Ar}^+/\text{cm}^2$ and $1 \times 10^{16} \text{ Ar}^+/\text{cm}^2$. At 648 K the corresponding values are $5.2 \text{ W/m} \cdot \text{K}$, $4.2 \text{ W/m} \cdot \text{K}$ and $2.5 \text{ W/m} \cdot \text{K}$ for the mentioned doses.²⁹

U_3O_8 was studied with different irradiation doses (from $0 \text{ Ar}^+/\text{cm}^2$ to $2 \times 10^{16} \text{ Ar}^+/\text{cm}^2$). Their thermal conductivities at 333 K are $1.67 \text{ W/m} \cdot \text{K}$ and $1.97 \text{ W/m} \cdot \text{K}$, respectively. The self-annealing is found to be stronger than in UO_2 , so that the thermal conductivities at 658 K are from $1.3 \text{ W/m} \cdot \text{K}$ and up to $1.86 \text{ W/m} \cdot \text{K}$, respectively, for the above-mentioned doses. For lower doses, the thermal conductivity decreases with increasing dose but then starts increasing again for higher doses. The possible cause of this effect might be related to re-crystallization and/or the formation of a second phase (e.g., UO_{2+x} in U_3O_8). In general, it was found that oxidation of UO_2 has a stronger influence on the thermal conductivity than irradiation with argon ions.²⁷

8. INTERACTIONS OF NUCLEAR FUEL WITH CLADDING MATERIAL

This is a complex topic that requires an in-depth study. Potential chemical interactions include: hydrogen uptake and oxidation (from the outside of the Zr-based cladding); irradiation-assisted corrosion phenomena, swelling of fuel with extended burn-up, and many other effects. In any case, it will be necessary to establish reliably the temperature distribution, neutron flux, fluence, chemical and phase composition of the selected zirconium based nuclear cladding alloy, as well as external pressure inside and outside a given fuel element. For all of these parameters, it is highly desirable to have not just averaged-out values, but the parameter field resolved in time and in space (for a given geometry of the fuel element).

As one of the preliminary steps in this work, we have calculated the phase composition as a function of temperature for all zirconium-based alloys considered for the TREAT fuel element cladding: Zircaloy-2; Zircaloy-4; ZIRLOTM; M5TM. These results are presented in Figure 12–Figure 15.^{28,29}

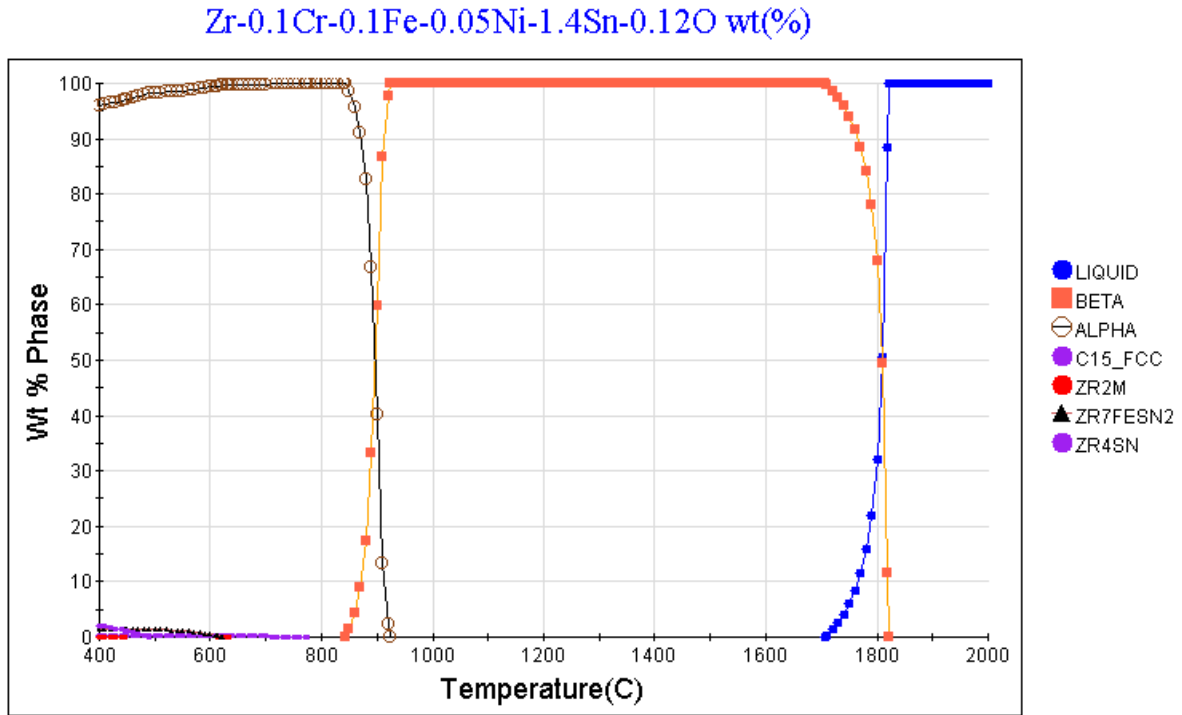


Figure 12. Temperature dependence of the phase composition for the alloy Zy-2.

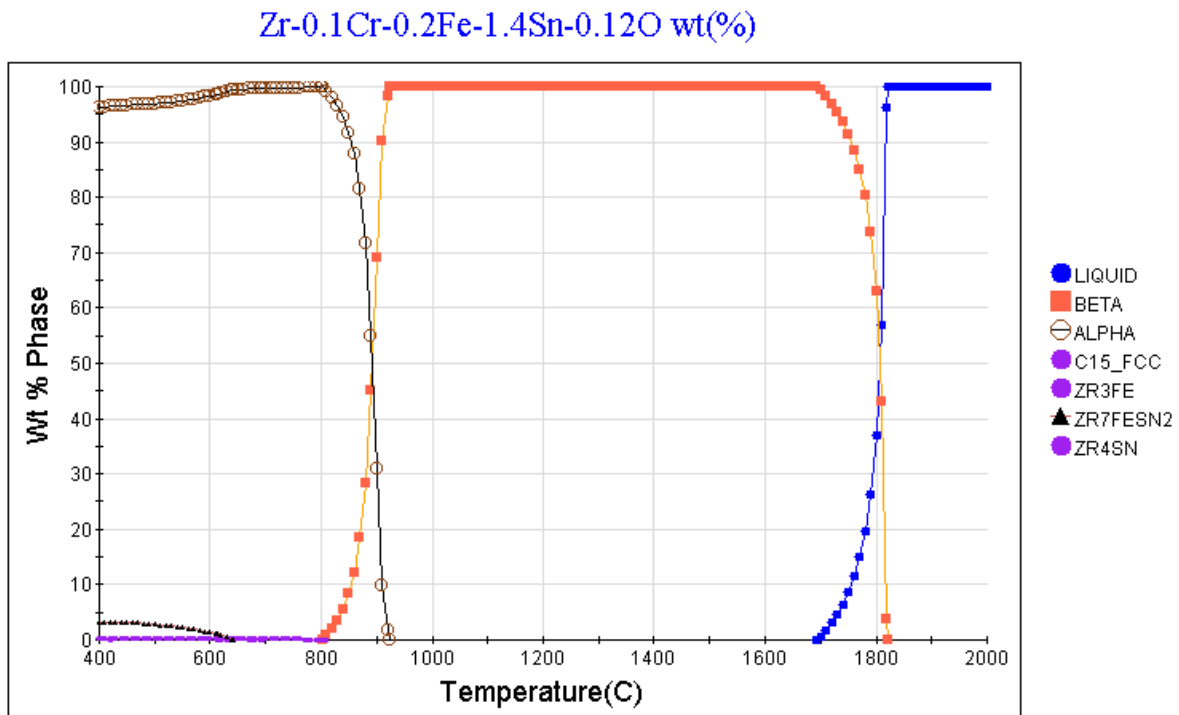


Figure 13. Temperature dependence of the phase composition for zircaloy-4.

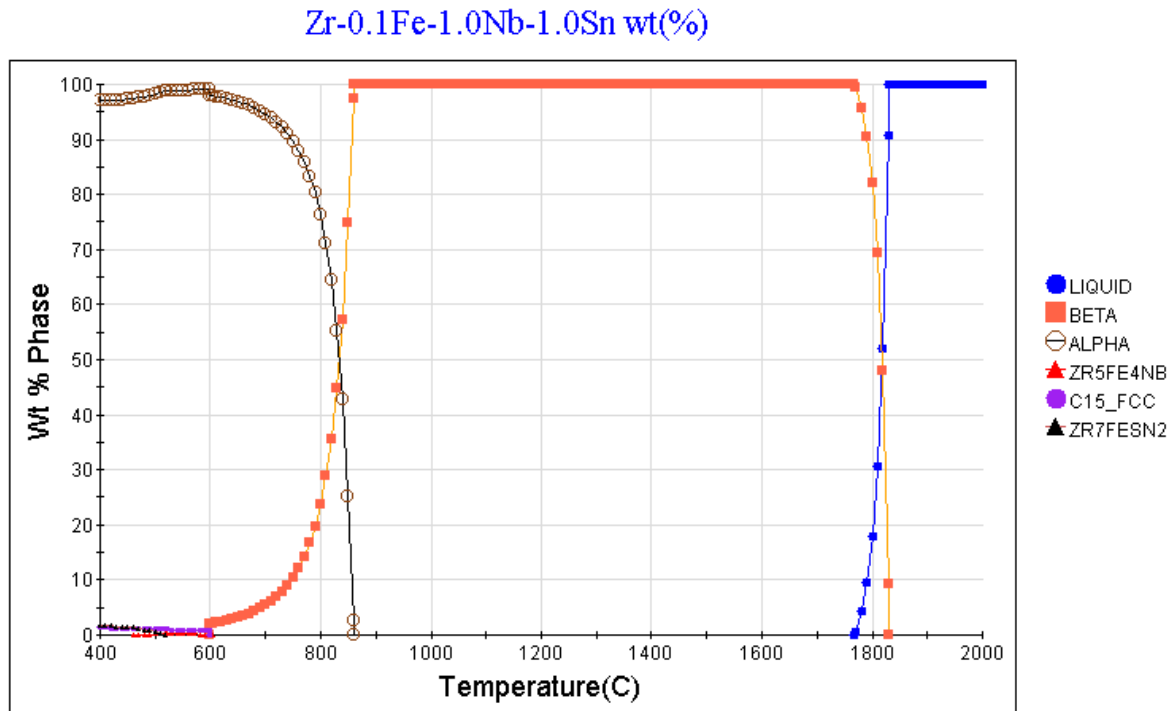


Figure 14. Temperature dependence of the phase composition for ZIRLO™.

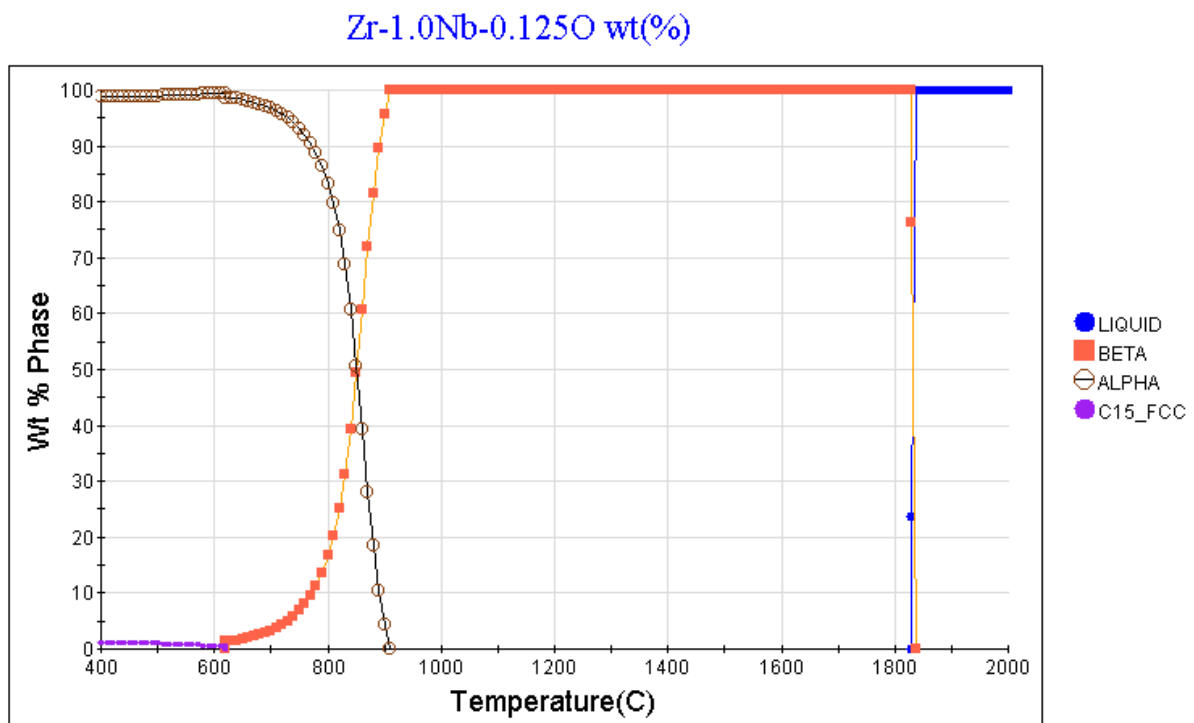


Figure 15. Temperature dependence of the phase composition for the alloy M5™.

Zircaloy-3 is an interesting material as well.²⁰ It contains about the same amount of iron as Zircaloy-4 (0.25%Fe), but no nickel, no chromium, and only a small amount of tin compared to all other zircalloys (0.25%). Its temperature dependence of the phase composition is provided in Figure 16.

Zr-0.25Fe-0.25Sn wt(%)

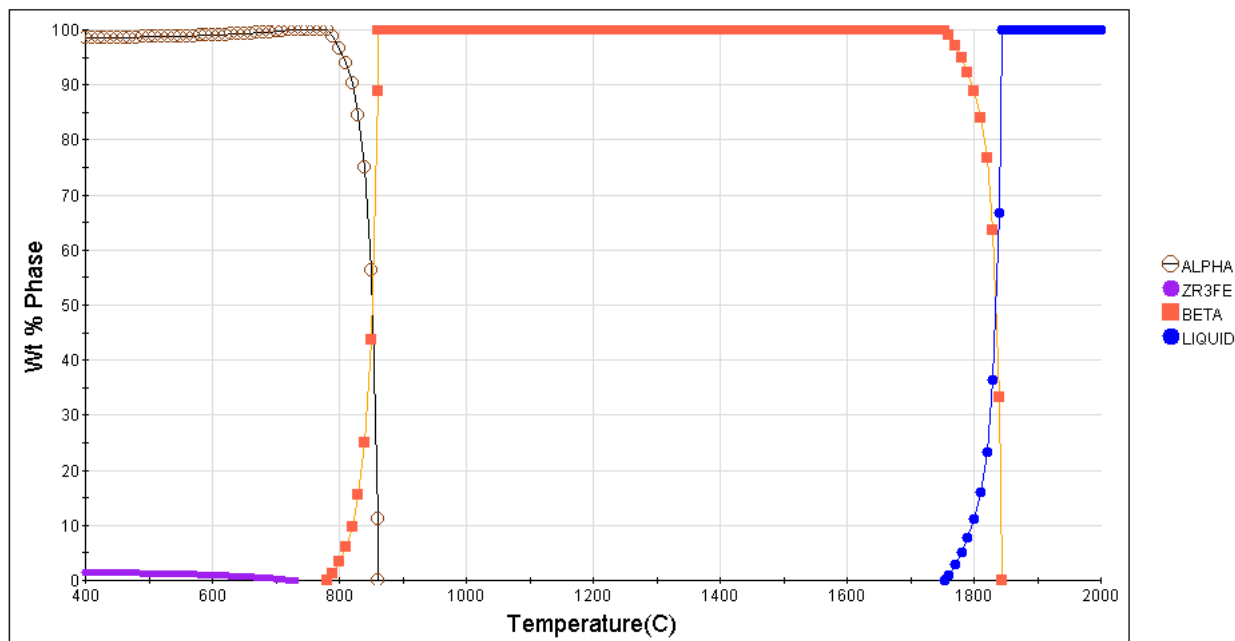


Figure 16. Temperature dependence of the phase composition for the alloy Zircaloy-3 (our calculations).

It is known from the literature^{23,24} that corrosion, mechanical, and thermo-physical properties of these materials can be changed in a favorable way by optimizing the so-called “temper” of these heat-treatable materials (via the construction of TTT- and CCT-diagrams). This work is planned for the future.

9. ACKNOWLEDGEMENTS

One of the authors (MVG) would like to express his sincere gratitude to Professor Indrajit Charit (University of Idaho, Moscow, ID) for his valuable thoughts and ideas shared during his presentation of the two classes “Nuclear Materials Science” and “Interaction of Radiation with Substance” in 2011-2012.

10. CONCLUSIONS

In this brief report, a preliminary conclusion (based upon both computational thermodynamics results of the authors and the literature analysis) was made for selecting UO_2 vs U_3O_8 as the nuclear fuel (to be dispersed in graphite) for the TREAT LEU fuel fabrication and reactor operational and accident conditions. The choice was made in favor of UO_2 for the following reasons:

1. UO_2 is exceptionally well-studied and understood, including its behavior in somewhat similar TRISO fuel
2. No phase transformations up to the point of congruent melting at the high temperature of $\sim 2850^\circ\text{C}$; the U-O and U-O-C phase diagrams are well understood
3. High symmetry of the UO_2 crystalline lattice and isotropy of properties in a broad temperature range ensure dimensional stability of fuel assemblies

4. While UO_2 may react with the graphite matrix forming UC_2 , for the U_3O_8 oxide, the onset of such chemical interactions takes place at lower temperatures (with all other factors being the same)
5. The issue of air ingress is well understood for UO_2 monolithic fuel, but not for the UO_2 fuel dispersed in the graphite matrix (see below)
6. It is important to understand the chemical reactivity mechanisms of UO_2 at elevated temperatures (corresponding to the RIA/LOCA incidents). This very important issue requires further study. However, using the thermodynamic calculations in this report, one can predict now that there will be competition for UO_2 in two major chemical processes corresponding to the above scenario: **reduction** of UO_2 by the graphite matrix accompanied by the formation of UC_2 and CO ; and **oxidation** of UO_2 to U_3O_8 by the ingress air. Furthermore, the onset temperatures for both processes are pressure-dependent. Of the two processes, the oxidation to U_3O_8 is probably the worst because it is accompanied by the specific volume change of about 38% and subsequent nonlinear oxide layer growth.³² Detailed experimentation and first-principles calculations could shed light upon this very complex issue. However, in terms of the possibility of a gap developing between the fuel and the carbon matrix, UO_2 is certainly preferable because its oxidation is accompanied by the specific volume growth accompanying the $\text{UO}_2 \rightarrow \text{U}_3\text{O}_8$ oxidative transformation.
7. While thermal conductivity of UO_2 and U_3O_8 is low, it is several times higher for UO_2 , although the exact ratio will be temperature-dependent.
8. Thermal expansion of UO_2 increases monotonically with temperature, changing $\sim 0.75\%$ in the 0°C - 1000°C temperature range. However, in the case of U_3O_8 the situation is more complex. Stoichiometric U_3O_8 changes continuously with increasing temperature, reversibly and anisotropically, above 25°C with expansion along the a-axis and contraction along the b-axis from orthorhombic to hexagonal symmetry at $350^\circ\text{C} \pm 10^\circ\text{C}$.²⁵ A small but continuous contraction along the c-axis occurs up to 1100°C . The loss of oxygen begins around 600°C . This does not result in any discontinuity in both parameters of the hexagonal phase (i.e., “a” and “c”) up to 875°C . However, in the range from 875°C to 925°C , the structure undergoes a change to lower symmetry as a result of contraction along the a-axis and expansion along the b-axis (expansion-contraction anomaly). This structural change is accompanied by a more extensive loss of oxygen and is usually irreversible. For these reasons, UO_2 is the oxide of choice from the thermal expansion behavior standpoint as well.

There are a number of things that still need to be explored further. One issue is the development of zirconium alloy tempering that would provide the best possible corrosion resistance for the selected Zr-based alloy (the construction of the TTT- and CCT-diagrams, analysis of mechanical behavior, selection of the optimal heat treatment, etc.). Secondly, the generalized Ellingham-Richardson diagram will need to be constructed for the zirconium alloy of choice in conditions of air ingress and at normal working conditions. Thirdly, to gain fundamental understanding of the UO_2 -graphite reactions, it is desirable to study the electronic density distributions for this reaction taking place under different conditions (density functional theory). Fourthly and finally, potential interactions between the fuel and the Zr-based cladding need to be understood in detail.

11. REFERENCES

1. I. J. van Rooyen, N. E. Woolstenhulme, R. K. Jamison, E. P. Luther, N. Valenti, TREAT Conversion LEU Fuel Design Trade Study, INL External Report INL/LTD-14-31704, Rev. 1, November 2015.
2. Transient Reactor Test Facility (TREAT) FSAR, Document ID: S3942-0001-YT, Revision ID: 8, Effective Date: 11/12/14.
3. Benjamin M. Ma, Nuclear Reactor Materials and Applications, 1st edition, Springer (1982).

4. K. Linga Murty and Indrajit Charit, Introduction to Nuclear Materials: Fundamentals and Applications, Wiley-VCH (2013).
5. S. M. Thein, P. J. Bereolos, Thermal Stabilization of $^{233}\text{UO}_2$, $^{233}\text{UO}_3$, and $^{233}\text{U}_3\text{O}_8$, ORNL/TM-2000/82, July 2000.
6. Steven C. Zumdahl, Chemical Principles, 6th Ed., Houghton Mifflin Company (2009).
[ISBN 0-618-94690-X](#).
7. S. G. Popov, J. J. Carbajo, V. K. Ivanov, G. L. Yoder, Thermophysical properties of MOX and UO_2 fuels including the effects of radiation, ORNL/TM-2000/351 (2000).
8. Leon C. Walters, Nuclear Fuel: Design and Fabrication, in Encyclopedia of Energy, vol. 4, pp. 341-350 (2004).
9. Dionissios Papadias, "Thermal Analysis of a TREAT Fuel Assembly," ANL/GTRI/TM-DRAFT, ANL Nuclear Engineering Division, July 9, 2014.
10. Thermo-Calc v.2015a, Stockholm, Sweden (2015).
11. Uranium Processing and Properties, edited by Jonathan S. Morrell, Mark J. Jackson, Springer, Berlin (2013).
12. M. T. Simnad, Nuclear Reactor Materials and Fuels, in: Encyclopedia of Physical Sciences and Technology, 3rd edition, vol.10, Academic Press (2002), pp.775-815.
13. Caneiro, A. and Abriata, J.P., Equilibrium Oxygen Partial Pressure and Phase Diagram of the Uranium-Oxygen System in the Composition Range $2.61 < \text{O/U} < 2.67$ between 844 and 1371 K, *Journal of Nuclear Materials* 126 (1984) 255-267.
14. Thompson W. T., Lewis B. J., Corcoran E. C., Kaye M. H., White S. J., Akbari F., He Z., Verrall R., Higgs J. D., Thompson D. M., Besmann T. M., and Vogel S. C., Thermodynamic treatment of uranium dioxide based nuclear fuel, *Int. J. Mater. Res.*, Vol. 98, 2007, p 1004-1011).
15. Bykov M. A., and Uspenskaya I. A., Thermodynamic Properties of Low-Stability Phases and the Phase Diagram of the Uranium-Oxygen System, *Zh. Neorg. Khim.*, Vol. 48, 2003, p. 1715-1717.
16. Rajendran Pillai S., Anthonysamy S., Prakashan P. K., Ranganathan R., Vasudeva Rao P. R., and Mathews C. K., Carburization of stainless steel clad by uranium-plutonium carbide fuel, *J. Nucl. Mater.*, vol. 167, 1989, p. 105-109.
17. https://en.wikipedia.org/wiki/Uranium_dioxide.
18. Indrajit Charit, Introduction to Nuclear Materials, University of Idaho (2012). Also see Reference 4.
19. Okamoto H., C-U (Carbon-Uranium), Binary Alloy Phase Diagrams, II Ed., Ed. T. B. Massalski, Vol. 1, 1990, p 892-893, *Journal of Chemistry*, Vol. 2015, Article ID 142510 (2015).
20. C. Duriez, M. Steinbrück, D. Ohai, T. Meleg, J. Birchley, T. Haste, Separate-effect tests on zirconium cladding degradation in air ingress situations, *Nucl. Engineering and Design* (2009).
21. G. W. Parker et al., "Out of Pile Studies of Fission-Product Release from Overheated Reactor Fuels at ORNL, 1955-1965," ORNL-3981 (July 1967).
22. F. C. Iglesias et al., "Measured Release Kinetics of Ruthenium from Uranium Oxides in Air," Proc. of Int. Seminar on Fission Product Transport Processes during Reactor Accidents, Editor J. T. Rogers, Hemisphere Publishing Corp, Washington DC (1990).
23. Jianguo Yu, Billy Valderrama, Hunter B. Henderson, Michele V. Manuel, and Todd Allen, Near Surface Stoichiometry in UO_2 : A Density Functional Theory Study, *Journal of Chemistry*, vol. 2015, Article No. 142510 (2015).

24. Thermal Conductivity of Uranium Dioxide, IAEA, Technical Report No. 59, Vienna (1965).
25. D. G. Martin, *Journal of Nuclear Materials*, vol.152, p.24 (1988).
26. M. Tokar et al., *Nuclear Technology*, vol.17, p.147 (1973).
27. C. G. S. Pillai, A. K. Dua, P. Raj, Thermal conductivity of U_3O_8 from 300 to 1100 K, *Journal of Nuclear Materials*, vol. 288, issues 2-3, pp. 87-91 (2001).
28. Patricia B. Weisensee, Thermal Conductivity of UO_2 and U_3O_8 Epitaxial Layers Damaged by Ion Irradiation, M.S. Thesis, University of Illinois, Urbana-Champaign (2011).
29. Glazoff, Michael V., Physical and Mechanical Metallurgy of Zirconium Alloys for Nuclear Applications: a Multi-Scale computational Study, Ph.D. Dissertation in Nuclear Engineering, the University of Idaho (Spring 2015). Advisor: Professor Akira Tokuhiro (now at Purdue University).
30. Glazoff, Michael V., Tokuhiro, Akira, Rashkeev, Sergey N., and Sabharwall, Piyush, Zirconium, Zircaloy-2, and Zircaloy-4: Computational Thermodynamics and Atomistic Perspective on Hydrogen Uptake and Oxidation, *Journal of Nuclear Materials*, vol. 444, pp. 65-75 (2014).
31. W. K. Anderson, C. J. Beck, A. R. Kephart, and J. S. Theilacker, Reactor Structural Materials: Engineering Properties as Affected by Nuclear Reactor Service, ASTM Special Technical Publication No. 314 (1962).
32. Nuclear Corrosion Science and Engineering, ed. By D. Feron, Woodhead Publishing Limited (2012).
33. B. Szpunar, J. A. Szpunar, V. Milman, A. Goldberg, Implication of volume changes in uranium oxides: A density functional study, *Solid State Sciences* vol. 24, pp. 44-53 (2013).